A COEFFICIENT MAKES SVRG EFFECTIVE

Anonymous authors
Paper under double-blind review

ABSTRACT

Stochastic Variance Reduced Gradient (SVRG), introduced by Johnson & Zhang (2013), is a theoretically compelling optimization method. However, as Defazio & Bottou (2019) highlight, its effectiveness in deep learning is yet to be proven. In this work, we demonstrate the potential of SVRG in optimizing real-world neural networks. Our empirical analysis finds that, for deeper neural networks, the strength of the variance reduction term in SVRG should be smaller and decrease as training progresses. Inspired by this, we introduce a multiplicative coefficient α to control the strength and adjust it through a linear decay schedule. We name our method α-SVRG. Our results show α-SVRG better optimizes models, consistently reducing training loss compared to the baseline and standard SVRG across various model architectures and multiple image classification datasets. We hope our findings encourage further exploration into variance reduction techniques in deep learning.

1 INTRODUCTION

A decade ago, Johnson & Zhang (2013) proposed a simple approach for reducing gradient variance in SGD – Stochastic Variance Reduced Gradient (SVRG). SVRG keeps a snapshot model and uses it to form a variance reduction term to adjust the gradient of the current model. This variance reduction term is the difference between the snapshot's stochastic gradient and its full gradient on the whole dataset. Utilizing this term, SVRG can reduce gradient variance of SGD and accelerate it to almost as fast as the full-batch gradient descent in strongly convex settings.

Over the years, numerous SVRG variants have emerged. Some focus on further accelerating convergence in convex settings (Xiao & Zhang, 2014; Lin et al., 2015; Defazio, 2016), while others are tailored for non-convex scenarios (Allen-Zhu & Hazan, 2016; Reddi et al., 2016; Lei et al., 2017; Fang et al., 2018). SVRG and its variants have shown effectiveness in optimizing simple machine learning models like logistic regression and ridge regression (Allen-Zhu, 2017; Lei et al., 2017).

Despite the theoretical value of SVRG and its subsequent works, they have seen limited practical success in training neural networks. Most SVRG research in non-convex settings is restricted to modest experiments: training basic models like Multi-Layer Perceptrons (MLP) or simple CNNs on small datasets like MNIST and CIFAR-10. These studies usually exclude evaluations on more capable and deeper networks. More recently, Defazio & Bottou (2019) have exploited several variance reduction methods, including SVRG, to deep vision models. They found that SVRG fails to reduce gradient variance for deep neural networks. This is because the model updates so quickly on the loss surface that the snapshot model becomes outdated and ineffective at variance reduction.

In this work, we show that adding a multiplicative coefficient to SVRG's variance reduction term can make it effective for deep neural networks. Our exploration is motivated by an intriguing observation: SVRG can only reduce gradient variance in the initial training stages but *increases* it later. To tackle this problem, we mathematically derive the optimal coefficient for the variance reduction term to minimize the gradient variance. Our empirical analysis then leads to two key observations about this optimal coefficient: (1) as the depth of the model increases, the optimal coefficient becomes smaller; (2) as training advances, the optimal coefficient decreases, dropping well below the default coefficient of 1 in SVRG. These findings help explain why a constant coefficient of 1 in SVRG, while initially effective, eventually fails to reduce gradient variance.

Based on these observations, we introduce a linearly decaying coefficient α to control the strength of the variance reduction term in SVRG. We call our method α-SVRG and illustrate it in Figure 1. α-SVRG decreases gradient variance stably across both early and late training and helps optimize

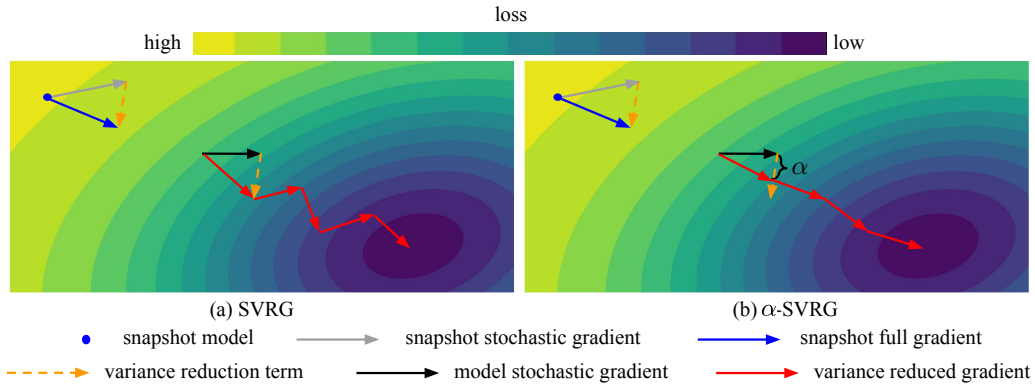

Figure 1: **SVRG vs. α-SVRG.** Both SVRG (left) and α-SVRG (right) use the difference between snapshot stochastic gradient (gray) and snapshot full gradient (blue) to form a variance reduction term (orange), which modifies model stochastic gradient (black) into variance reduced gradient (red). But α-SVRG employs a coefficient α to modulate the strength of the variance reduction term. With this coefficient, α-SVRG reduces the gradient variance and results in faster convergence.

the model better. We evaluate α-SVRG on a range of architectures and image classification datasets. α-SVRG achieves a lower training loss than the baseline and the standard SVRG. Our results highlight the value of SVRG in deep learning. We hope our work can offer insights about SVRG and stimulate more research in variance reduction approaches for optimization in neural networks.

2 Motivation: SVRG may not always reduce variance

SVRG formulation. We first introduce the basic formulation of SVRG. We adopt the following notation: t is the iteration index, $\boldsymbol{\theta}^t$ represents the current model parameters, and $\nabla f_i(\cdot)$ denotes the gradient of loss function f for the i-th mini-batch. In SVRG's original work (Johnson & Zhang, 2013), this corresponds to the i-th data point. When the subscript i is omitted, $\nabla f(\cdot)$ represents the full gradient across the entire dataset. A key concept in SVRG is the snapshot model, represented as $\boldsymbol{\theta}^{\text{past}}$. It is a snapshot of the model at a previous iteration before t. We store its full gradient $\nabla f(\boldsymbol{\theta}^{\text{past}})$. This snapshot is taken periodically. SVRG defines the variance reduced gradient $\boldsymbol{g}_i^t$, as follows:

$$\boldsymbol{g}_i^t = \nabla f_i(\boldsymbol{\theta}^t) - \underbrace{\left(\nabla f_i(\boldsymbol{\theta}^{\text{past}}) - \nabla f(\boldsymbol{\theta}^{\text{past}})\right)}_{\text{variance reduction term}}. \tag{1}$$

Intuitively, SVRG uses the difference between the mini-batch gradient and full gradient of a past model to modify the current mini-batch gradient. This could make $\boldsymbol{g}_i^t$ better aligned with the current full gradient $\nabla f(\boldsymbol{\theta}^t)$ and thus stabilize each update.

SVRG was initially introduced in the context of vanilla SGD. Recent work (Dubois-Taine et al., 2021; Wang & Klabjan, 2022) has integrated SVRG into alternative base optimizers. Following them, we input the variance reduced gradient $\boldsymbol{g}_i^t$ into the base optimizer. Also, SVRG uses the same base optimizer as baseline and takes snapshot once per training epoch following (Defazio & Bottou, 2019).

Gradient variance. Our goal is to assess SVRG's effectiveness in reducing gradient variance. To this end, we gather N mini-batch gradients, denoted as $\{\boldsymbol{g}_i^t | i \in \{1, \cdots, N\}\}$, by performing back-propagation on checkpoints of the model at the iteration t with randomly selected N mini-batches. For SVRG, each gradient is modified based on Equation 1. To present a comprehensive view, we employ three metrics from prior studies to quantify gradient variance in Table 1.

Here, we discuss each metric in detail. Metric 1 calculates the cosine distance between pairwise mini-batch gradients. Thus, it only captures variance in gradient directions and disregards variance in gradient magnitudes. This is very important for scale-invariant modern optimizers, such as Adagrad (Lydia & Francis, 2019) and Adam (Kingma & Ba, 2015). In contrast, metric 2 focuses on both gradient directions and magnitudes by summing the variance of each component of gradients. This metric has been the standard tool to measure gradient variance in various optimization literature (Allen-Zhu & Hazan, 2016; Defazio & Bottou, 2019). Metric 3 considers the largest eigenvalue of gradient covariance matrix, characterizing the most dominant part in gradient variance.

name	formula	description
metric 1	$\frac{2}{N(N-1)} \sum_{i \neq j} \frac{1}{2}(1 - \frac{\langle \boldsymbol{g}_i^t, \boldsymbol{g}_j^t \rangle}{\|\boldsymbol{g}_i^t\|_2 \|\boldsymbol{g}_j^t\|_2})$	the directional variance of the gradients
metric 2	$\sum_{k=1}^{d} \mathrm{Var}(g_{i,k}^t)$	the variance of gradients across each component
metric 3	$\lambda_{max}(\frac{1}{N} \sum_{i=1}^{N} (\boldsymbol{g}_i^t - \boldsymbol{g}^t)(\boldsymbol{g}_i^t - \boldsymbol{g}^t)^T)$	the magnitude of the most significant variation

Table 1: **Metrics.** $\boldsymbol{g}^t$ is the mean of the gradients $\boldsymbol{g}_i^t$. k indexes the k-th component of gradient $g_{i,k}^t$.

Despite great differences in these metrics, they exhibit consistent trends when comparing different optimization methods. Our following experiments will further illustrate the reliability of these metrics.

SVRG's effect on gradient variance. To understand how SVRG affects training, we examine two simple models: a linear layer (Logistic Regression) and a 4-layer Multi-Layer Perceptron (MLP-4). We train them over 30 epochs on CIFAR-10. We compare SVRG to a baseline using only SGD.

We plot Logistic Regression's gradient variance (top two and bottom left) and training loss (bottom right) in Figure 2. For Logistic Regression, SVRG can reduce the gradient variance throughout the entire training process and achieve a lower training loss than the baseline.

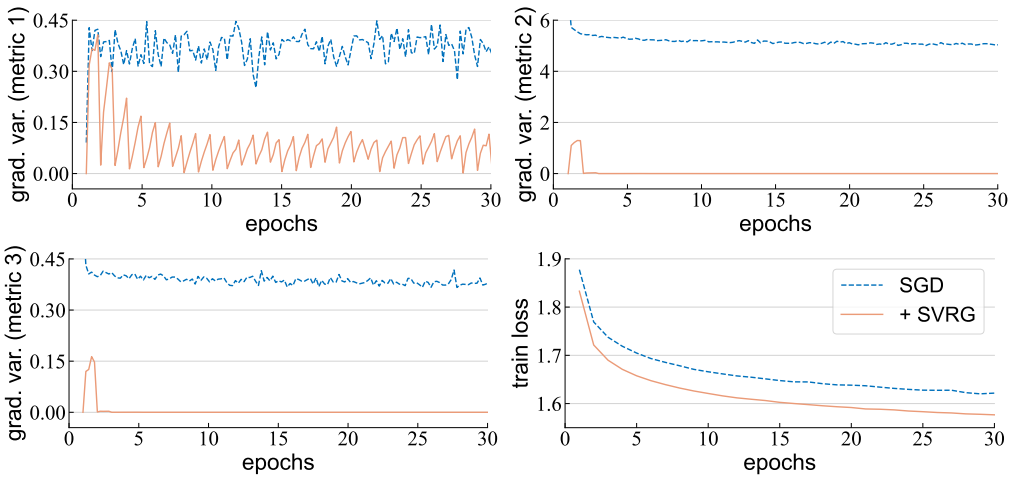

Figure 2: **SVRG on Logistic Regression.** SVRG effectively reduces the gradient variance for Logistic Regression, leading to a lower training loss than the baseline.

In contrast, for MLP-4, SVRG may not always reduce gradient variance. As shown in Figure 3, SVRG can only decrease the gradient variance for the first five epochs but then increases it. Consequently,

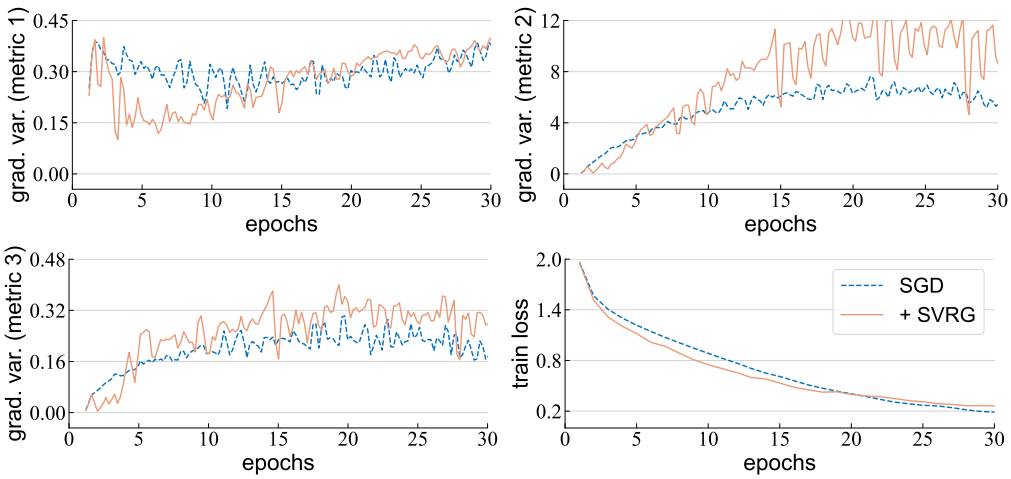

Figure 3: **SVRG on MLP-4.** In the first few epochs, SVRG reduces the gradient variance for MLP-4, but afterward, SVRG increases it, well above the baseline. As a result, SVRG exhibits a higher training loss than the baseline at the end of training.

SVRG has a larger final training loss than the baseline. This indicates the increase in gradient variance caused by SVRG hinders the convergence of MLP-4's training loss.

This surprising empirical observation in a slightly deeper model leads us to question whether SVRG may alter the gradient too excessively at certain phases of training. Can we mitigate this adverse effect? We explore these questions starting from a theoretical framework in the next section.

3 A Closer Look at Control Variates in SVRG

Control variates (Lavenberg et al., 1977) is a technique initially developed in Monte Carlo methods to reduce variance. We aim to estimate the expected value of a random variable X. The variance of this estimate usually depends on $\mathrm{Var}(\mathrm{X})$. To form a less variate estimate X^*, we can use a control variate Y that correlates with X and a coefficient α to regulate the influence of Y and $\mathbb{E}[\mathrm{Y}]$:

$$\mathrm{X}^* = \mathrm{X} - \alpha(\mathrm{Y} - \mathbb{E}[\mathrm{Y}]). \tag{2}$$

This estimate remains unbiased for any value of α. The coefficient that minimizes the variance of the estimate can be derived as:

$$\alpha^* = \frac{\mathrm{Cov}(\mathrm{X}, \mathrm{Y})}{\mathrm{Var}(\mathrm{Y})} = \rho(\mathrm{X}, \mathrm{Y})\frac{\sigma(\mathrm{X})}{\sigma(\mathrm{Y})}, \tag{3}$$

where $\rho(\mathrm{X}, \mathrm{Y})$ represents the correlation coefficient between X and Y; $\sigma(\cdot)$ denotes the standard deviation. The derivation is detailed in Appendix A. The minimized variance becomes $\mathrm{Var}(\mathrm{X}^*) = (1 - \rho(\mathrm{X}, \mathrm{Y})^2)\mathrm{Var}(\mathrm{X})$. The higher the correlation is, the lower the variance of the estimate is.

Note that SVRG uses control variates to reduce variance in each component of the gradient. This variance reduction occurs at each iteration t. Take a closer look at Equation 1 and 2: the model stochastic gradient $f_i(\boldsymbol{\theta}^t)$ is the random variable X; the snapshot stochastic gradient $f_i(\boldsymbol{\theta}^{\text{past}})$ is the control variate Y; and the snapshot full gradient $f(\boldsymbol{\theta}^{\text{past}})$ is the expectation $\mathbb{E}[\mathrm{Y}]$.

A key difference between SVRG and control variates is that SVRG omits the coefficient α, defaulting it to 1. This is possibly because the gradient distribution does not change drastically in strongly convex settings. Yet, SVRG's subsequent studies, even those addressing non-convex cases, have neglected the coefficient and formulated their theories based on Equation 1.

Motivated by this, we introduce a time-dependent coefficient vector $\boldsymbol{\alpha}^t \in \mathbb{R}^d$ in SVRG:

$$\boldsymbol{g}_i^t = \nabla f_i(\boldsymbol{\theta}^t) - \boldsymbol{\alpha}^t \odot (\nabla f_i(\boldsymbol{\theta}^{\text{past}}) - \nabla f(\boldsymbol{\theta}^{\text{past}})), \tag{4}$$

where $\odot$ represents the element-wise multiplication.

Optimal coefficient. We adopt the same gradient variance definition as Defazio & Bottou (2019) (metric 2 in Table 1) and aim to determine the optimal $\boldsymbol{\alpha}^{t*}$ that minimizes it at each iteration. Specifically, our objective is to minimize the sum of variances across each component of $\boldsymbol{g}_i^t$. Let k index the k-th component α_k^{t*} and the k-th component of the gradient $\nabla f_{\cdot,k}(\cdot)$. For clarity, we omit the mini-batch index i. This can be formally expressed as follows:

$$\min_{\boldsymbol{\alpha}^t} \sum_{k=1}^{d} \mathrm{Var}(g_{\cdot,k}^t) = \sum_{k=1}^{d} \min_{\alpha_k^t} \mathrm{Var}(g_{\cdot,k}^t). \tag{5}$$

We can switch the order of minimization and summation in Equation 5 because the variance of the k-th component of the gradient only depends on the k-th component of the coefficient. Applying Equation 3 yields the optimal coefficient α_k^{t*}:

$$\alpha_k^{t*} = \frac{\mathrm{Cov}(\nabla f_{\cdot,k}(\boldsymbol{\theta}^{\text{past}}), \nabla f_{\cdot,k}(\boldsymbol{\theta}^t))}{\mathrm{Var}(\nabla f_{\cdot,k}(\boldsymbol{\theta}^{\text{past}}))} = \rho(\nabla f_{\cdot,k}(\boldsymbol{\theta}^{\text{past}}), \nabla f_{\cdot,k}(\boldsymbol{\theta}^t))\frac{\sigma(\nabla f_{\cdot,k}(\boldsymbol{\theta}^t))}{\sigma(\nabla f_{\cdot,k}(\boldsymbol{\theta}^{\text{past}}))}. \tag{6}$$

A stronger correlation between the snapshot and model gradients leads to a larger optimal coefficient.

For small networks like MLP-4, calculating the optimal coefficient at each iteration is feasible by gathering all mini-batch gradients for both the current and snapshot models. For larger networks, however, this method becomes impractical; we will address this challenge later in the paper.

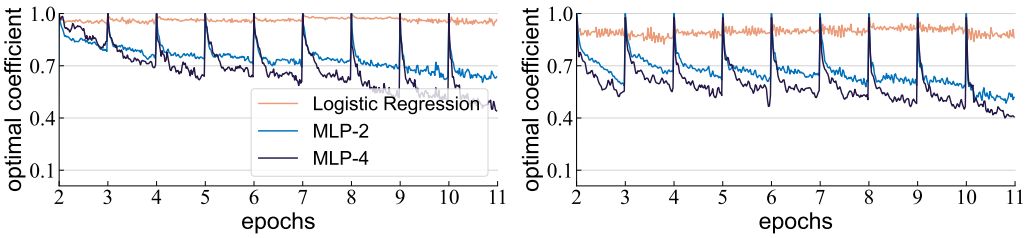

(a) SGD (b) AdamW

Figure 4: **Optimal coefficient.** At the start of each epoch, a snapshot is taken. Consequently, the optimal coefficient initiates at a value of 1 and results in a periodic upward jump.

Observations on optimal coefficient. To explore how the optimal coefficient evolves in a normal training setting, we train 1, 2, and 4-layer MLPs (Logistic Regression, MLP-2, and MLP-4) using SGD and AdamW (Loshchilov & Hutter, 2019) on CIFAR-10 *without using SVRG*. Given the small size of these models, we can analytically compute the optimal coefficient at each iteration. We plot its mean value over all indices k in Figure 4. We can make two notable observations as below.

Observation 1: a deeper model has a smaller optimal coefficient. For Logistic Regression, the optimal coefficient remains relatively stable, hovering near 1. For MLP-2, the coefficient deviates from 1, dropping to about 0.6. For MLP-4, it decreases more sharply, reaching approximately 0.4.

Observation 2: the average optimal coefficient of a deeper model in each epoch generally decreases as training progresses. This suggests that each epoch's average correlation between snapshot gradients and model gradients ($\rho(\nabla f_{\cdot,k}(\boldsymbol{\theta}^{\text{past}}), \nabla f_{\cdot,k}(\boldsymbol{\theta}^t))$ in Equation 6) decreases as the model becomes better trained. We further analyze this decreasing trend of the correlation term in Appendix E.

These observations shed light on why the standard SVRG struggles to reduce gradient variance or training loss in later training stages (Figure 3). A default coefficient of 1 proves to be too high and the weakening correlation between snapshot and model gradients necessitates a smaller coefficient. Without a suitable coefficient, gradient variance may increase, leading to oscillations in SGD.

Optimal coefficient's effect on gradient variance. We evaluate whether optimal coefficient can make SVRG more effective in reducing gradient variance. Specifically, we use SVRG with optimal coefficient to train an MLP-4 by computing optimal coefficient (Equation 6) and adjusting the gradient (Equation 4) at each iteration. In Figure 5, we compare SVRG with optimal coefficient to an SGD baseline. Using the optimal coefficient enables SVRG to reduce gradient variance in the early stages of training without uplifting it later. This yields a consistently lower training loss than the baseline.

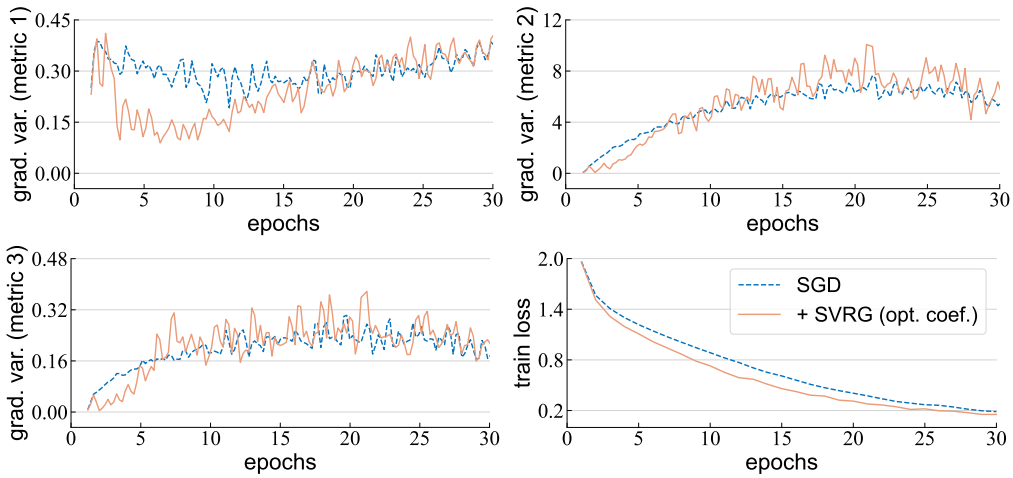

Figure 5: **SVRG with optimal coefficient on MLP-4.** SVRG with the optimal coefficient reduces gradient variance stably and achieves a lower training loss than the baseline SGD.

4 α-SVRG

From our analysis above, it becomes clear that the best coefficient for SVRG is not necessarily 1 for deep neural networks. However, computing the optimal coefficient at each iteration would result in a complexity of full-batch gradient descent. This approach quickly becomes impractical for larger networks like ResNet (He et al., 2016). In this section, we show how using a preset schedule of α values can achieve a similar effect of using the computed optimal coefficients.

α-SVRG. Given the decreasing trend (Figure 4) and the computational challenge, we propose to apply a linearly decreasing scalar coefficient (more in Section 5.3) for SVRG, starting from an initial value α_0 and decreasing to 0. This is our main method in this paper. We name it α-SVRG. The convergence analysis of α-SVRG is available in Appendix G

To evaluate how well α-SVRG matches SVRG with optimal coefficient, we train an MLP-4 using α-SVRG and compare it to SVRG with optimal coefficient. For all experiments in this section, we set $\alpha_0 = 0.5$. The results are presented in Figure 6. Interestingly, α-SVRG exhibits a gradient variance trend that is not much different from SVRG with optimal coefficient. Similarly, the training loss of α-SVRG is only marginally larger than that of SVRG with optimal coefficient.

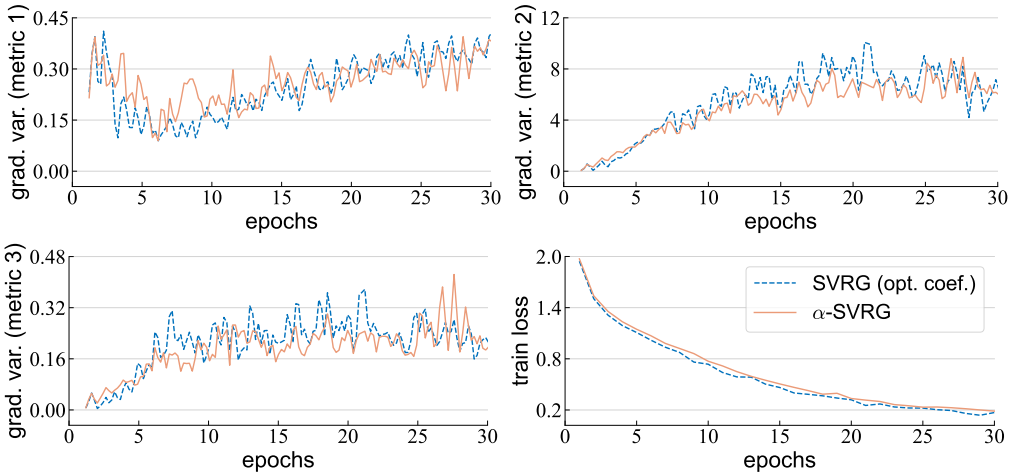

Figure 6: **α-SVRG on MLP-4.** α-SVRG behaves similarly to SVRG with optimal coefficient.

α-SVRG with AdamW. Since AdamW (Loshchilov & Hutter, 2019) is a widely used optimizer in modern neural network training, we assess the performance of α-SVRG with AdamW. We change the base optimizer in α-SVRG to AdamW and use it to train an MLP-4 on CIFAR-10. We compare α-SVRG to a baseline using only AdamW. Figure 7 shows the results. α-SVRG has a gradient variance reduction and achieves a consistent lower training loss for MLP-4 than the baseline.

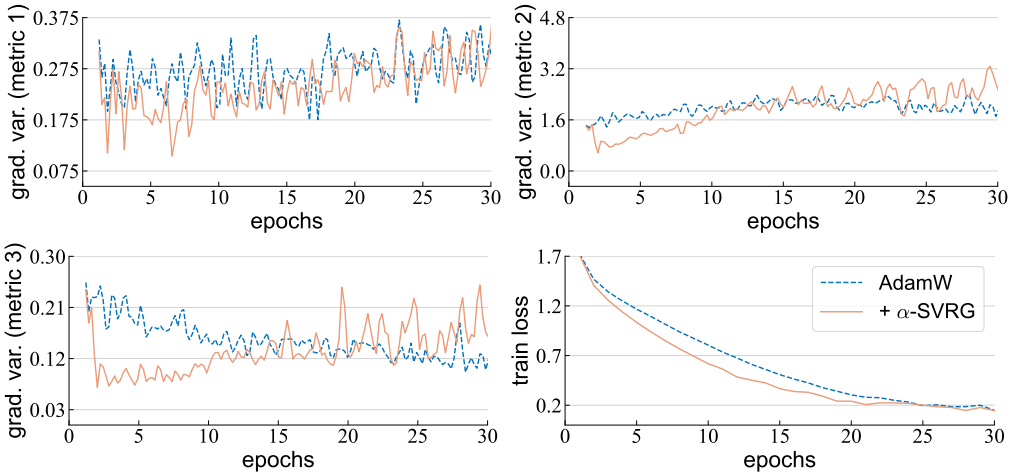

Figure 7: **α-SVRG with AdamW on MLP-4**. α-SVRG can lower the gradient variance at the first 10 epochs, leading to a faster convergence than the baseline AdamW.

α-SVRG on deeper networks. We further study the effectiveness of α-SVRG with AdamW on real-world neural architectures, moving beyond simple MLPs. To this end, we train a modern ConvNet architecture, ConvNeXt-Femto (Liu et al., 2022; Wightman, 2019), on CIFAR-10 using the default AdamW optimizer. We compare α-SVRG to the baseline using vanilla AdamW in Figure 8.

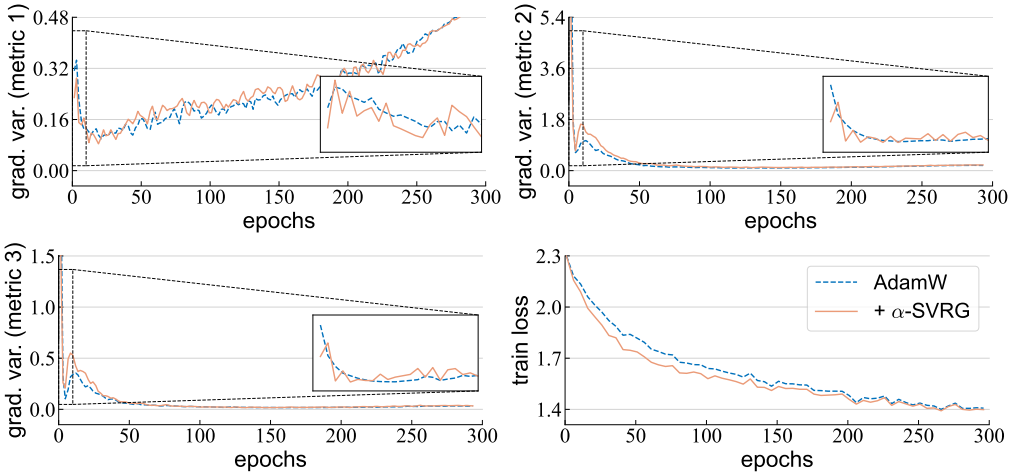

Figure 8: **α-SVRG on ConvNeXt-Femto**. α-SVRG can reduce the gradient variance for ConvNeXt-Femto during the first 10 epochs (zoom-in plot) without increasing it later on. Consequently, α-SVRG can decrease the training loss at a faster rate than the baseline AdamW.

α-SVRG can reduce gradient variance during the first 10 epochs (zoom-in plot of Figure 8) and then maintain it at the same level as the baseline. As a result, the training loss of α-SVRG converges much faster than the baseline. This demonstrates the potential of α-SVRG in optimizing more complex models. We further explore this with additional experiments next.

5 Experiments

5.1 Settings

Datasets. We evaluate α-SVRG using ImageNet-1K classification (Deng et al., 2009) as well as smaller image classification datasets: CIFAR-100 (Krizhevsky, 2009), Flowers (Nilsback & Zisserman, 2008), Pets (Parkhi et al., 2012), STL-10 (Coates et al., 2011), Food-101 (Bossard et al., 2014), DTD (Cimpoi et al., 2014), SVHN (Netzer et al., 2011), and EuroSAT (Helber et al., 2019).

Models. We use recently proposed vision models on ImageNet-1K, categorized into two groups: (1) smaller models with 5-19M parameters, including ConvNeXt-F (Wightman, 2019; Liu et al., 2022), ViT-T/16 (Dosovitskiy et al., 2021), Swin-F (Liu et al., 2021b), and Mixer-S/32 (Tolstikhin et al., 2021); (2) larger models featuring 86M and 89M parameters: ViT-B/16 and ConvNeXt-B. ConvNeXt-F is also evaluated on all smaller image classification datasets.

Training. We report both final training loss and top-1 validation accuracy. Our basic training setting follows ConvNeXt (Liu et al., 2022), which uses AdamW. Both SVRG and α-SVRG also use AdamW as the base optimizer. On small datasets, we choose the best α_0 from $\{0.5, 0.75, 1\}$. We find the coefficient is robust and does not require extensive tuning. Therefore, for ImageNet-1K, we set α_0 to 0.75 for smaller models and 0.5 for larger ones. Other training settings for α-SVRG remain the same as the baseline. Further experimental settings can be found in Appendix B.

5.2 Results

Table 2 presents the results of training various models on ImageNet-1K. The standard SVRG often increases the training loss, especially for larger models. In contrast, α-SVRG decreases the training loss for both smaller and larger models. This also supports our earlier finding that deeper models benefit from lower coefficient values and using a default coefficient of 1 impedes convergence.

	ConvNeXt-F		ViT-T		Swin-F		Mixer-S		ViT-B		ConvNeXt-B	
					training loss							
AdamW	3.487	-	3.443	-	3.427	-	3.149	-	2.817	-	2.644	-
+ SVRG	3.505	↑.018	3.431	↓.012	**3.389**	↓.038	3.172	↑.023	3.309	↑.492	3.113	↑.469
+ α-SVRG	**3.471**	↓.016	**3.415**	↓.028	3.392	↓.035	**3.097**	↓.052	**2.806**	↓.011	**2.642**	↓.002
					validation accuracy							
AdamW	76.0	-	73.9	-	74.3	-	**76.4**	-	**81.6**	-	**83.7**	-
+ SVRG	75.7	↓0.3	**74.3**	↑0.4	74.3	↑0.0	74.5	↓1.9	78.0	↓3.6	80.8	↓2.9
+ α-SVRG	**76.3**	↑0.3	74.2	↑0.3	**74.8**	↑0.5	76.1	↓0.3	**81.6**	↑0.0	83.1	↓0.6

Table 2: **Results on ImageNet-1K.** The standard SVRG increases the training loss for most models, whereas α-SVRG consistently decreases it for all models.

	CIFAR-100		Pets		Flowers		STL-10		Food-101		DTD		SVHN		EuroSAT	
							training loss									
AdamW	2.66	-	2.20	-	2.40	-	1.64	-	2.45	-	1.98	-	1.59	-	1.25	-
+ SVRG	2.94	↑0.28	3.42	↑1.22	2.26	↓0.14	1.90	↑0.26	3.03	↑0.58	2.01	↑0.03	1.64	↑0.05	1.25	0.00
+ α-SVRG	**2.62**	↓0.04	**1.96**	↓0.24	**2.16**	↓0.24	**1.57**	↓0.07	**2.42**	↓0.03	**1.83**	↓0.15	**1.57**	↓0.02	**1.23**	↓0.02
							validation accuracy									
AdamW	81.0	-	72.8	-	80.8	-	82.3	-	**85.9**	-	57.9	-	94.9	-	98.1	-
+ SVRG	78.2	↓2.8	17.6	↓55.2	82.6	↑1.8	65.1	↓17.2	79.6	↓6.3	57.8	↓0.1	95.7	↑0.8	97.9	↓0.2
+ α-SVRG	**81.4**	↑0.4	**77.8**	↑5.0	**83.3**	↑2.5	**84.0**	↑1.7	**85.9**	↑0.0	**61.8**	↑3.9	**95.8**	↑0.9	**98.2**	↑0.1

Table 3: **Results on smaller classification datasets.** While the standard SVRG mostly hurts the performance, α-SVRG decreases the training loss and increases the validation accuracy.

Table 3 displays the results of training ConvNeXt-F on various smaller datasets. The standard SVRG generally elevates the training loss and impairs the generalization. On the contrary, α-SVRG lowers the training loss and improves the validation accuracy across all small datasets. Full results of α-SVRG with different initial coefficient on smaller classification datasets are in Appendix C.

Note that a lower training loss in α-SVRG does not always lead to better generalization. For smaller models, a lower training loss usually directly translates to a higher validation accuracy. In larger models (Mixer-S, ViT-B, and ConvNeXt-B), additional adjustments to regularization strength may be needed for better generalization. This is out of scope for α-SVRG as an optimization method but warrants future research on co-adapting optimization and regularization.

We have included more experiments and visualizations in Appendix. In Appendix F, we demonstrate the advantage gained from α-SVRG is statistically significant compared with other optimizers. In Appendix H, we include more qualitative convergence comparisons between AdamW and α-SVRG.

5.3 Analysis on Coefficient Scheduling Strategies

Notations. For clarity, we decompose the global iteration index t into an epoch-wise index s and an iteration index i within an epoch. We also denote the total number of training epochs as T and represent the number of iterations in one epoch as M.

Linear schedule. Throughout the paper, we employ a coefficient that decays linearly across epochs and keeps as a constant within an epoch for α-SVRG:

$$\alpha^t_{\text{linear}} = \alpha_0(1 - \frac{s(t)}{T}), \tag{7}$$

Other global schedules. Nevertheless, there are other potential decaying schedules, such as quadratic decay or geometric decay. They can be formally expressed as:

$$\alpha^t_{\text{quadratic}} = \frac{\alpha_0}{T^2}(T - s(t))^2, \tag{8}$$

$$\alpha^t_{\text{geometric}} = \alpha_0(\frac{10^{-2}}{\alpha_0})^{\frac{s(t)}{T}}. \tag{9}$$

Double schedules. In Figure 4, within each epoch, the coefficient also starts from 1 and decreases over iterations. Motivated by this local behavior, we introduce three additional schedules that combine both the local and global decay: d(ouble)-linear, d-quadratic, and d-geometric. In addition to the global decay, each double schedule has another local decay for each epoch that initiates at 1 and decreases to an ending value specified by the global decay.

$$\alpha^t_{\text{d-linear}} = \alpha^t_{\text{linear}} \underbrace{(1 - \frac{i}{M})}_{\text{local decay}} + \alpha^t_{\text{linear}} \tag{10}$$

$$\alpha^t_{\text{d-quadratic}} = (1 - \alpha^t_{\text{quadratic}}) \underbrace{\frac{1}{M^2}(M - i)^2}_{\text{local decay}} + \alpha^t_{\text{quadratic}} \tag{11}$$

$$\alpha^t_{\text{d-geometric}} = \underbrace{(\alpha^t_{\text{geometric}} + 10^{-2})^{\frac{i}{M}}}_{\text{local decay}} \tag{12}$$

We provide visualizations of three global schedules and three double schedules in Appendix D.

Results. We evaluate these six schedules with three different initial coefficients α_0 from $\{0.5, 0.75, 1\}$ by training ConvNeXt-Femto on STL-10. Table 4 presents the results. α-SVRG with double schedules surprisingly have a higher training loss than the AdamW baseline (1.641). This is possibly because the coefficient within an epoch sometimes overestimates the optimal coefficient and therefore increases gradient variance. In contrast, α-SVRG with global schedules consistently achieves a lower training loss than the baseline (1.641) regardless of the choice of any initial coefficient.

train loss	linear	quadratic	geometric	d-linear	d-quadratic	d-geometric
$\alpha_0 = 0.5$	**1.583**	1.607	1.616	2.067	1.967	1.808
$\alpha_0 = 0.75$	**1.568**	1.576	1.582	2.069	2.003	1.931
$\alpha_0 = 1$	1.573	**1.563**	1.574	1.997	1.970	1.883

Table 4: **Schedules.** α-SVRG with global schedules outperforms that with double schedules.

5.4 Analysis

We analyze various components in α-SVRG. In the following experiments, we use an initial value $\alpha_0 = 0.5$ and ConvNeXt-F on STL-10 as the default setting. Because the standard SVRG is ineffective here as discussed above, we omit it and only compare α-SVRG to an AdamW baseline.

Coefficient value. We investigate the impact of the initial value of the coefficient α_0 for α-SVRG. We vary it between 0 and 1 and observe its effect on the training loss. The results are presented in Figure 9. The favorable range for initial values in α-SVRG is quite broad, ranging from 0.2 to 0.9. This robustness indicates α-SVRG requires minimal tuning in the practical setting.

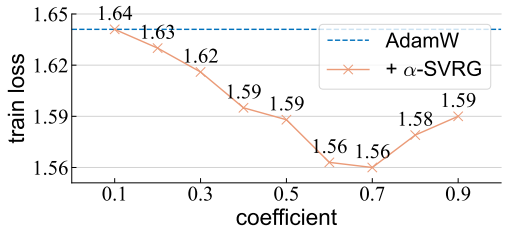

Figure 9: **Coefficient value.** α-SVRG is effective with a wide range of coefficient values.

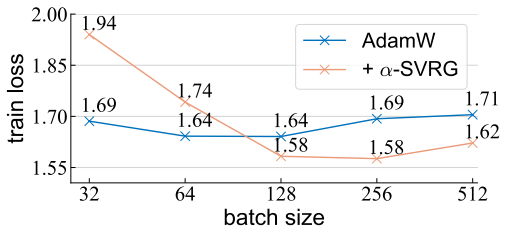

Figure 10: **Batch size.** α-SVRG's effectiveness is observed for larger batch sizes.

Batch size. Since the batch size controls the variance among mini-batch data, we change the batch size to understand how it affects α-SVRG. We also scale the learning rate linearly (Goyal et al., 2017). The default batch size is 128. In Figure 10, we can see that α-SVRG leads to a lower training loss when the batch size is larger, but it is worse than the baseline when the batch size is smaller. This may stem from the weakening correlation between snapshot gradients and model gradients as the batch size decreases. Therefore, a sufficiently large batch size is essential for α-SVRG.

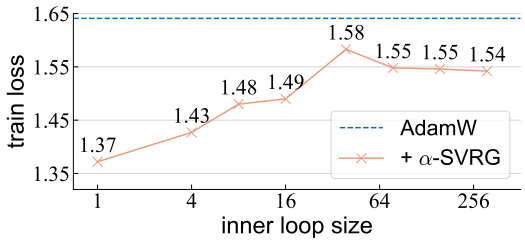

Figure 11: **Inner loop size.** Although a greater inner loop size leads to a weakening correlation between the model gradients and the snapshot gradients, α-SVRG can still lower the training loss.

Inner Loop Size. The inner loop size specifies the number of iterations between two consecutive snapshot captures. We vary it from 1 to 312 iterations to understand its effect on α-SVRG. The default value is 39 iterations (one epoch). Figure 11 illustrates α-SVRG has a lower training loss than the baseline even with a larger inner loop size, where the snapshot is relatively distant from the current model. On the other hand, a smaller inner loop size results in a lower training loss but requires additional training time, as a full gradient must be calculated each time a snapshot is taken.

6 Related Work

Variance reduction in optimization. There are a range of methods aiming at reducing gradient variance by directly modifying stochastic gradient. Initial works (Johnson & Zhang, 2013; Schmidt et al., 2016) focus on simple convex settings. Subsequent research enhances these methods (Defazio et al., 2014a; Mairal, 2015; Babanezhad Harikandeh et al., 2015; Lin et al., 2015; Defazio, 2016; Allen-Zhu, 2017; Lin et al., 2018; Sebbouh et al., 2019) or handles finite sums in non-convex landscapes (Allen-Zhu & Hazan, 2016; Reddi et al., 2016; Nguyen et al., 2017; Fang et al., 2018; Li & Li, 2018; Cutkosky & Orabona, 2019; Wang et al., 2019; Elibol et al., 2020; Kavis et al., 2022). For these methods, we either need to store all gradient with respect to each individual data point (Defazio et al., 2014b; Shalev-Shwartz & Zhang, 2013; Li et al., 2021) or calculate full gradient periodically (Johnson & Zhang, 2013; Fang et al., 2018; Li et al., 2021). Gower et al. (2020) provide a comprehensive review for variance reduction methods. While these studies focus more on theories of SVRG, we primarily explore the practical utility of SVRG for real-world neural networks.

Implicit variance reduction. Apart from methods that explicitly adjust the gradient, there are variance reduction techniques that implicitly reduce gradient variance through other means. A variety of optimizers (Zeiler, 2012; Kingma & Ba, 2015; Dozat, 2016; Lydia & Francis, 2019; Loshchilov & Hutter, 2019; Liu et al., 2021a; 2024; Chen et al., 2023) utilize momentum to mitigate gradient variance. They achieve this by averaging past gradients exponentially, thus stabilizing subsequent updates. Lookahead optimizer (Zhang et al., 2019) reduces gradient variance by only updating the model once every k iterations. Dropout (Hinton et al., 2012) is also found to reduce gradient variance and better optimize models when used at early training (Liu et al., 2023).

7 Conclusion

Over the past decade, SVRG has been a method with a significant impact on the theory of optimization. In this work, we explore the effectiveness of SVRG in training real-world neural networks. Our key insight is the optimal strength for the variance reduction term in SVRG is not necessarily 1. It should be lower for deeper networks and decrease as training advances. This motivates us to introduce α-SVRG: applying a linearly decreasing coefficient α to SVRG. α-SVRG leads to a steady reduction in gradient variance and optimizes models better. Our experiments show that α-SVRG consistently achieves a lower training loss compared to both baseline and the standard SVRG. Our results motivate further research of variance reduction methods in neural networks training.

Reproducibility Statement: We document our training recipe and hyper-parameter selections in detail in Appendix B. Our code could be found in the anonymous GitHub repository: https://github.com/abc-092/alpha-SVRG. It is also included in the supplementary material.

REFERENCES

Zeyuan Allen-Zhu. Katyusha: The first direct acceleration of stochastic gradient methods. *Symposium on Theory of Computing*, 2017.

Zeyuan Allen-Zhu and Elad Hazan. Variance reduction for faster non-convex optimization. In *ICML*, 2016.

Reza Babanezhad Harikandeh, Mohamed Osama Ahmed, Alim Virani, Mark Schmidt, Jakub Konečný, and Scott Sallinen. Stopwasting my gradients: Practical svrg. In *NeurIPS*, 2015.

Lukas Bossard, Matthieu Guillaumin, and Luc Van Gool. Food-101–mining discriminative components with random forests. In *ECCV*, 2014.

Xiangning Chen, Chen Liang, Da Huang, Esteban Real, Kaiyuan Wang, Yao Liu, Hieu Pham, Xuanyi Dong, Thang Luong, Cho-Jui Hsieh, Yifeng Lu, and Quoc Le. Symbolic discovery of optimization algorithms. *arXiv preprint arXiv:2302.06675*, 2023.

Mircea Cimpoi, Subhransu Maji, Iasonas Kokkinos, Sammy Mohamed, and Andrea Vedaldi. Describing textures in the wild. In *CVPR*, 2014.

Adam Coates, Andrew Ng, and Honglak Lee. An analysis of single-layer networks in unsupervised feature learning. In *AISTATS*, 2011.

Ekin Cubuk, Barret Zoph, Jonathon Shlens, and Quoc Le. Randaugment: Practical automated data augmentation with a reduced search space. In *CVPR Workshops*, 2020.

Ashok Cutkosky and Francesco Orabona. Momentum-based variance reduction in non-convex sgd. In *NeurIPS*, 2019.

Alex Damian, Tengyu Ma, and Jason D Lee. Label noise sgd provably prefers flat global minimizers. In *NeurIPS*, 2021.

Aaron Defazio. A simple practical accelerated method for finite sums. In *NeurIPS*, 2016.

Aaron Defazio and Lon Bottou. On the ineffectiveness of variance reduced optimization for deep learning. *arXiv preprint arXiv:1812.04529*, 2019.

Aaron Defazio, Francis Bach, and Simon Lacoste-Julien. Saga: A fast incremental gradient method with support for non-strongly convex composite objectives. In *NeurIPS*, 2014a.

Aaron Defazio, Tibrio Caetano, and Justin Domke. Finito: A faster, permutable incremental gradient method for big data problems. In *ICML*, 2014b.

Jia Deng, Wei Dong, Richard Socher, Li-Jia Li, Kai Li, and Li Fei-Fei. ImageNet: A large-scale hierarchical image database. In *CVPR*, 2009.

Alexey Dosovitskiy, Lucas Beyer, Alexander Kolesnikov, Dirk Weissenborn, Xiaohua Zhai, Thomas Unterthiner, Mostafa Dehghani, Matthias Minderer, Georg Heigold, Sylvain Gelly, Jakob Uszkoreit, and Neil Houlsby. An image is worth 16x16 words: Transformers for image recognition at scale. In *ICLR*, 2021.

Timothy Dozat. Incorporating Nesterov Momentum into Adam. In *ICLR*, 2016.

Benjamin Dubois-Taine, Sharan Vaswani, Reza Babanezhad, Mark Schmidt, and Simon Lacoste-Julien. Svrg meets adagrad: Painless variance reduction. *arXiv preprint arXiv:2102.09645*, 2021.

Melih Elibol, Lihua Lei, and Michael Jordan. Variance reduction with sparse gradients. In *ICLR*, 2020.

Cong Fang, Chris Junchi Li, Zhouchen Lin, and Tong Zhang. Spider: Near-optimal non-convex optimization via stochastic path integrated differential estimator. In *NeurIPS*, 2018.

Robert Gower, Mark Schmidt, Francis Bach, and Peter Richtrik. Variance-reduced methods for machine learning. In *IEEE*, 2020.

Priya Goyal, Piotr Dollár, Ross Girshick, Pieter Noordhuis, Lukasz Wesolowski, Aapo Kyrola, Andrew Tulloch, Yangqing Jia, and Kaiming He. Accurate, large minibatch SGD: Training ImageNet in 1 hour. *arXiv preprint arXiv:1706.02677*, 2017.

Kaiming He, Xiangyu Zhang, Shaoqing Ren, and Jian Sun. Deep residual learning for image recognition. In *CVPR*, 2016.

Patrick Helber, Benjamin Bischke, Andreas Dengel, and Damian Borth. Eurosat: A novel dataset and deep learning benchmark for land use and land cover classification. *IEEE Journal of Selected Topics in Applied Earth Observations and Remote Sensing*, 2019.

Geoffrey Hinton, Nitish Srivastava, Alex Krizhevsky, Ilya Sutskever, and Ruslan R Salakhutdinov. Improving neural networks by preventing co-adaptation of feature detectors. *arXiv preprint arXiv:1207.0580*, 2012.

Gao Huang, Yu Sun, Zhuang Liu, Daniel Sedra, and Kilian Q Weinberger. Deep networks with stochastic depth. In *ECCV*, 2016.

Rie Johnson and Tong Zhang. Accelerating stochastic gradient descent using predictive variance reduction. In *NeurIPS*, 2013.

Ali Kavis, Stratis Skoulakis, Kimon Antonakopoulos, Leello Tadesse Dadi, and Volkan Cevher. Adaptive stochastic variance reduction for non-convex finite-sum minimization. In *NeurIPS*, 2022.

Diederik Kingma and Jimmy Ba. Adam: A method for stochastic optimization. In *ICLR*, 2015.

Alex Krizhevsky. Learning multiple layers of features from tiny images. *Tech Report*, 2009.

Stephen Lavenberg, Thomas L Moeller, and Peter D Welch. The application of control variables to the simulation of closed queueing networks. In *Proceedings of the 9th conference on Winter simulation-Volume 1*, 1977.

Lihua Lei, Cheng Ju, Jianbo Chen, and Michael Jordan. Non-convex finite-sum optimization via scsg methods. In *NeurIPS*, 2017.

Zhiyuan Li, Tianhao Wang, and Sanjeev Arora. What happens after sgd reaches zero loss? –a mathematical framework. In *ICLR*, 2022.

Zhize Li and Jian Li. A simple proximal stochastic gradient method for nonsmooth nonconvex optimization. In *NeurIPS*, 2018.

Zhize Li, Slavomír Hanzely, and Peter Richtárik. Zerosarah: Efficient nonconvex finite-sum optimization with zero full gradient computation. *arXiv preprint arXiv:2103.01447*, 2021.

Hongzhou Lin, Julien Mairal, and Zaid Harchaoui. A universal catalyst for first-order optimization. In *NeurIPS*, 2015.

Hongzhou Lin, Julien Mairal, and Zaid Harchaoui. Catalyst acceleration for first-order convex optimization: from theory to practice. *JMLR*, 2018.

Hong Liu, Zhiyuan Li, David Hall, Percy Liang, and Tengyu Ma. Sophia: A scalable stochastic second-order optimizer for language model pre-training. In *ICLR*, 2024.

Liyuan Liu, Haoming Jiang, Pengcheng He, Weizhu Chen, Xiaodong Liu, Jianfeng Gao, and Jiawei Han. On the variance of the adaptive learning rate and beyond. In *ICLR*, 2021a.

Ze Liu, Yutong Lin, Yue Cao, Han Hu, Yixuan Wei, Zheng Zhang, Stephen Lin, and Baining Guo. Swin transformer: Hierarchical vision transformer using shifted windows. In *ICCV*, 2021b.

Zhuang Liu, Hanzi Mao, Chao-Yuan Wu, Christoph Feichtenhofer, Trevor Darrell, and Saining Xie. A convnet for the 2020s. In *CVPR*, 2022.

Zhuang Liu, Zhiqiu Xu, Joseph Jin, Zhiqiang Shen, and Trevor Darrell. Dropout reduces underfitting. In *ICML*, 2023.

Ilya Loshchilov and Frank Hutter. Decoupled weight decay regularization. In *ICLR*, 2019.

Agnes Lydia and Sagayaraj Francis. Adagradan optimizer for stochastic gradient descent. *JMLR*, 2019.

Julien Mairal. Incremental majorization-minimization optimization with application to large-scale machine learning. *SIAM Journal on Optimization*, 2015.

Yuval Netzer, Tao Wang, Adam Coates, Alessandro Bissacco, Bo Wu, and Andrew Ng. Reading digits in natural images with unsupervised feature learning. In *NIPS Workshop*, 2011.

Lam Nguyen, Jie Liu, Katya Scheinberg, and Martin Tak. Sarah: A novel method for machine learning problems using stochastic recursive gradient. In *ICML*, 2017.

Maria-Elena Nilsback and Andrew Zisserman. Automated flower classification over a large number of classes. In *Indian Conference on Computer Vision, Graphics & Image Processing*, 2008.

Omkar Parkhi, Andrea Vedaldi, Andrew Zisserman, and CV Jawahar. Cats and dogs. In *CVPR*, 2012.

Sashank Reddi, Ahmed Hefny, Suvrit Sra, Barnabas Poczos, and Alex Smola. Stochastic variance reduction for nonconvex optimization. In *ICML*, 2016.

Mark Schmidt, Nicolas Le Roux, and Francis Bach. Minimizing finite sums with the stochastic average gradient. *arXiv preprint arXiv:1309.2388*, 2016.

Othmane Sebbouh, Nidham Gazagnadou, Samy Jelassi, Francis Bach, and Robert Gower. Towards closing the gap between the theory and practice of svrg. In *NeurIPS*, 2019.

Shai Shalev-Shwartz and Tong Zhang. Stochastic dual coordinate ascent methods for regularized loss minimization. *JMLR*, 2013.

Samuel Smith, Erich Elsen, and Soham De. On the generalization benefit of noise in stochastic gradient descent. In *ICML*, 2020.

Christian Szegedy, Vincent Vanhoucke, Sergey Ioffe, Jonathon Shlens, and Zbigniew Wojna. Rethinking the inception architecture for computer vision. In *CVPR*, 2016.

Ilya Tolstikhin, Neil Houlsby, Alexander Kolesnikov, Lucas Beyer, Xiaohua Zhai, Thomas Unterthiner, Jessica Yung, Andreas Steiner, Daniel Keysers, Jakob Uszkoreit, Mario Lucic, and Alexey Dosovitskiy. Mlp-mixer: An all-mlp architecture for vision. In *NeurIPS*, 2021.

Ruiqi Wang and Diego Klabjan. Divergence results and convergence of a variance reduced version of adam. *arXiv preprint arXiv:2210.05607*, 2022.

Zhe Wang, Kaiyi Ji, Yi Zhou, Yingbin Liang, and Vahid Tarokh. Spiderboost and momentum: Faster stochastic variance reduction algorithms. In *NeurIPS*, 2019.

Ross Wightman. GitHub repository: Pytorch image models. *GitHub repository*, 2019.

Lin Xiao and Tong Zhang. A proximal stochastic gradient method with progressive variance reduction. *SIAM Journal on Optimization*, 2014.

Sangdoo Yun, Dongyoon Han, Seong Joon Oh, Sanghyuk Chun, Junsuk Choe, and Youngjoon Yoo. Cutmix: Regularization strategy to train strong classifiers with localizable features. In *ICCV*, 2019.

Matthew Zeiler. Adadelta: An adaptive learning rate method. *arXiv preprint arXiv:1212.5701*, 2012.

Hongyi Zhang, Moustapha Cisse, Yann Dauphin, and David Lopez-Paz. mixup: Beyond empirical risk minimization. In *ICLR*, 2018.

Michael Zhang, James Lucas, Geoffrey Hinton, and Jimmy Ba. Lookahead optimizer: k steps forward, 1 step back. In *NeurIPS*, 2019.

Zhun Zhong, Liang Zheng, Guoliang Kang, Shaozi Li, and Yi Yang. Random erasing data augmentation. In *AAAI*, 2020.

APPENDIX

A DERIVATION OF THE OPTIMAL COEFFICIENT

We present the full derivation of the optimal coefficient for control variates:

$$\min_{\alpha} \mathrm{Var}(\mathrm{X}^*) = \min_{\alpha} \mathrm{Var}(\mathrm{X} - \alpha \mathrm{Y}) \tag{13}$$

$$= \min_{\alpha} \mathrm{Var}(\mathrm{X}) - 2\alpha \mathrm{Cov}(\mathrm{X}, \mathrm{Y}) + \alpha^2 \mathrm{Var}(\mathrm{Y}). \tag{14}$$

Differentiating the objective with respect to α, we can determine the optimal coefficient α^*:

$$2\alpha \mathrm{Var}(\mathrm{Y}) - 2\mathrm{Cov}(\mathrm{X}, \mathrm{Y}) = 0, \tag{15}$$

$$\implies \alpha^* = \frac{\mathrm{Cov}(\mathrm{X}, \mathrm{Y})}{\mathrm{Var}(\mathrm{Y})}. \tag{16}$$

Lastly, we can plug the definition of the correlation coefficient:

$$\rho(\mathrm{X}, \mathrm{Y}) = \frac{\mathrm{Cov}(\mathrm{X}, \mathrm{Y})}{\sigma(\mathrm{X})\sigma(\mathrm{Y})} \tag{17}$$

into the optimal coefficient and rewrite Equation 16 as:

$$\alpha^* = \rho(\mathrm{X}, \mathrm{Y}) \frac{\sigma(\mathrm{X})}{\sigma(\mathrm{Y})}. \tag{18}$$

B EXPERIMENTAL SETTINGS

Training recipe. Table 5 outlines our training recipe. It is based on the setting in ConvNeXt (Liu et al., 2022). For all experiments, the base learning rate is set at 4e-3, except for training ConvNeXt-F on ImageNet-1K using α-SVRG, where increasing it to 8e-3 reduces training loss very much.

Training Setting	Configuration
weight init	trunc. normal (0.2)
optimizer	AdamW
base learning rate	4e-3
weight decay	0.05
optimizer momentum	$\beta_1, \beta_2 = 0.9, 0.999$
learning rate schedule	cosine decay
warmup schedule	linear
randaugment (Cubuk et al., 2020)	(9, 0.5)
mixup (Zhang et al., 2018)	0.8
cutmix (Yun et al., 2019)	1.0
random erasing (Zhong et al., 2020)	0.25
label smoothing (Szegedy et al., 2016)	0.1

Table 5: **Our basic training recipe,** adapted from ConvNeXt (Liu et al., 2022).

Hyperparameters. Table 6 lists the batch size, warmup epochs, and training epochs for each dataset. Note the hyperparameters selections are done on the baseline. For each dataset, we set the batch size

	CIFAR-100	Pets	Flowers	STL-10	Food101	DTD	SVHN	EuroSAT	ImageNet-1K
batch size	1024	128	128	128	1024	128	1024	512	4096
warmup epochs	50	100	100	50	50	100	20	40	50
training epochs	300	600	600	300	300	600	100	200	300

Table 6: **Hyper-parameter setting.**

proportional to its total size and tune the training epochs to achieve reasonable performance with the AdamW baseline. The warmup epochs are set to one-fifth or one-sixth of the total training epochs.

We do not use stochastic depth (Huang et al., 2016) on small models. For larger models, we adhere to the original work (Dosovitskiy et al., 2021; Liu et al., 2022), using a stochastic depth rate of 0.4 for ViT-B and 0.5 for ConvNeXt-B. In these models, we maintain a consistent stochastic pattern between the current model and the snapshot at each iteration (Defazio & Bottou, 2019).

C Different Initial Coefficients

Table 7 presents the performance of ConvNeXt-F trained with α-SVRG using different initial coefficients α_0 on various image classification datasets. α-SVRG consistently reduces the training loss of ConvNeXt-F and enhances the validation accuracy on most datasets, regardless of the choice of initial coefficient α_0. This demonstrates the robustness of α-SVRG to the initial coefficient.

	CIFAR-100		Pets		Flowers		STL-10	
AdamW	2.659	-	2.203	-	2.400	-	1.641	-
+ SVRG	2.937	↑0.278	3.424	↑1.221	2.256	↓0.144	1.899	↑0.258
+ α-SVRG ($\alpha_0 = 0.5$)	**2.622**	↓0.037	1.960	↓0.243	2.265	↓0.135	1.583	↓0.058
+ α-SVRG ($\alpha_0 = 0.75$)	2.646	↓0.013	2.004	↓0.199	**2.162**	↓0.238	**1.568**	↓0.073
+ α-SVRG ($\alpha_0 = 1$)	2.712	↑0.053	**1.994**	↓0.209	2.259	↓0.141	1.573	↓0.068
	Food-101		DTD		SVHN		EuroSAT	
AdamW	2.451	-	1.980	-	1.588	-	1.247	-
+ SVRG	3.026	↑0.575	2.009	↑0.029	1.639	↑0.051	1.249	↑0.002
+ α-SVRG ($\alpha_0 = 0.5$)	**2.423**	↓0.028	1.865	↓0.115	**1.572**	↓0.016	1.243	↓0.004
+ α-SVRG ($\alpha_0 = 0.75$)	2.461	↑0.010	1.829	↓0.151	1.573	↓0.015	1.237	↓0.010
+ α-SVRG ($\alpha_0 = 1$)	2.649	↑0.198	**1.790**	↓0.190	1.585	↓0.003	**1.230**	↓0.017

(a) **training loss**

	CIFAR-100		Pets		Flowers		STL-10	
AdamW	81.0	-	72.8	-	80.8	-	82.3	-
+ SVRG	78.2	↓2.8	17.6	↓55.2	82.6	↑1.8	65.1	↓17.2
+ α-SVRG ($\alpha_0 = 0.5$)	**81.4**	↑0.4	**77.8**	↑5.0	**83.3**	↑2.5	**83.5**	↑1.2
+ α-SVRG ($\alpha_0 = 0.75$)	80.6	↓0.4	76.7	↑3.9	82.6	↑1.8	84.0	↑1.7
+ α-SVRG ($\alpha_0 = 1$)	80.0	↓1.0	77.3	↑4.5	81.9	↑1.1	84.0	↑1.7
	Food-101		DTD		SVHN		Euro	
AdamW	**85.9**	-	57.9	-	94.9	-	98.1	-
+ SVRG	79.6	↓6.3	57.8	↓0.1	95.7	↑0.8	97.9	↓0.2
+ α-SVRG ($\alpha_0 = 0.5$)	**85.9**	↑0.0	57.0	↓0.9	95.4	↑0.5	**98.2**	↑0.1
+ α-SVRG ($\alpha_0 = 0.75$)	85.0	↓0.9	60.3	↑2.4	95.7	↑0.8	**98.2**	↑0.1
+ α-SVRG ($\alpha_0 = 1$)	83.8	↓2.1	**61.8**	↑3.9	**95.8**	↑0.9	**98.2**	↑0.1

(b) **validation accuracy**

Table 7: **Results on smaller classification datasets with different initial coefficients.** While SVRG negatively affects performance on most of these datasets, α-SVRG consistently reduces the training loss and improves the validation accuracy for almost any initial coefficient on each dataset.

D VISUALIZATION OF DIFFERENT COEFFICIENT SCHEDULES

In Section 5.3, we propose six different ways to schedule coefficients in α-SVRG. We illustrate each of six coefficient schedules (with an initial coefficient of $\alpha_0 = 1$) over 10 epochs in Figure 12.

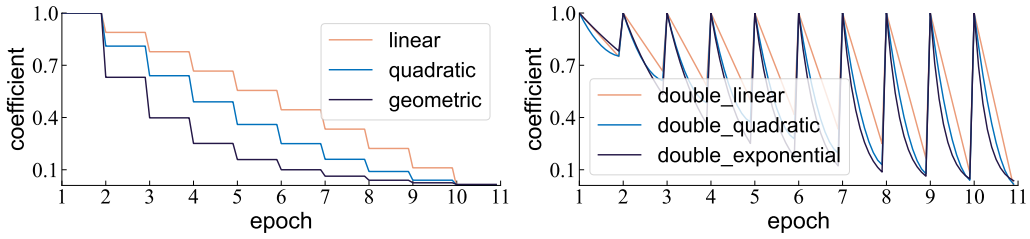

(a) global schedules (b) double schedules

Figure 12: **Different coefficient schedules.** Each global schedule (left) maintains a static coefficient within an epoch and applies a coefficient decay only at the end of each epoch. In contrast, each double schedule (right) also adjusts the coefficient within an epoch.

E CORRELATION BETWEEN MODEL GRADIENTS AND SNAPSHOT GRADIENTS

In Section 3, we find each epoch's average optimal coefficient decreases as training progresses. Here, we separately plot the standard deviation ratio $\frac{\sigma(\nabla f_{\cdot,k}(\boldsymbol{\theta}_t^s))}{\sigma(\nabla f_{\cdot,k}(\boldsymbol{\theta}^{\text{past}}))}$ in Figure 13 and the correlation $\rho(\nabla f_{\cdot,k}(\boldsymbol{\theta}^{\text{past}}), \nabla f_{\cdot,k}(\boldsymbol{\theta}_t^s))$ in Figure 14.

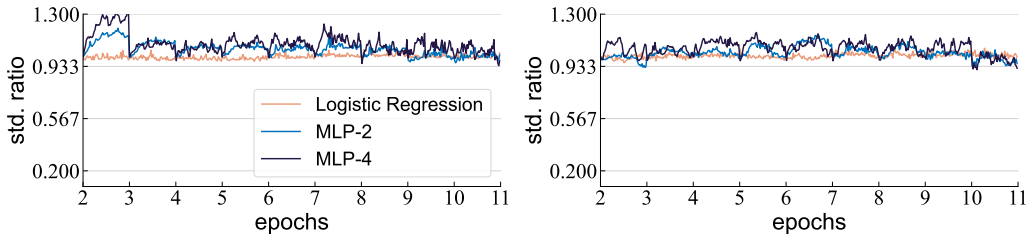

(a) SGD (b) AdamW

Figure 13: **Standard deviation ratio.** The ratio between the standard deviations of the model gradients and the snapshot gradients oscillates around 1 but is relatively stable overall.

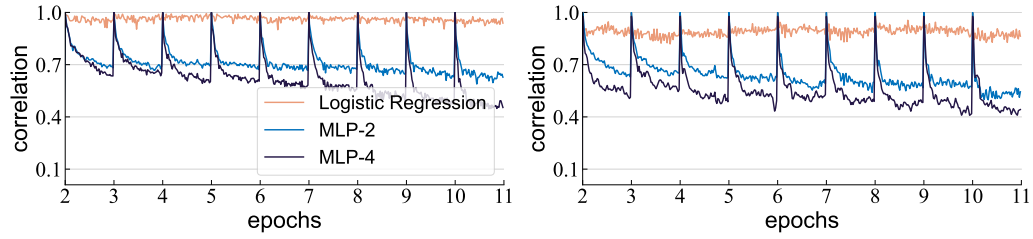

(a) SGD (b) AdamW

Figure 14: **Correlation.** The correlation between the snapshot gradients and the model gradients behaves very similarly to the optimal coefficient.

F STANDARD DEVIATION RESULTS

We run the baseline and α-SVRG in Table 3 with 3 random seeds. Table 8 presents the results. α-SVRG decreases the mean training loss and improves the mean validation accuracy. The mean difference is usually larger than one standard deviation, indicating the reliability of α-SVRG.

	CIFAR-100	Pets	Flowers	STL-10
AdamW	2.645 ± 0.013	2.326 ± 0.088	2.436 ± 0.038	1.660 ± 0.017
+ α-SVRG	**2.606** ± 0.017	**2.060** ± 0.071	**2.221** ± 0.042	**1.577** ± 0.022
	Food-101	DTD	SVHN	EuroSAT
AdamW	2.478 ± 0.021	2.072 ± 0.066	1.583 ± 0.005	1.259 ± 0.017
+ α-SVRG	**2.426** ± 0.007	**1.896** ± 0.075	**1.572** ± 0.011	**1.239** ± 0.016

(a) **training loss**

	CIFAR-100	Pets	Flowers	STL-10
AdamW	81.02 ± 0.07	70.61 ± 1.55	80.33 ± 1.01	80.80 ± 1.46
+ α-SVRG	**81.07** ± 0.22	**76.37** ± 1.06	**84.15** ± 1.15	**83.65** ± 0.92
	Food-101	DTD	SVHN	EuroSAT
AdamW	85.29 ± 0.47	56.21 ± 1.19	94.29 ± 0.67	97.91 ± 0.12
+ α-SVRG	**85.45** ± 0.43	**61.44** ± 0.35	**94.94** ± 0.60	**98.13** ± 0.07

(b) **validation accuracy**

Table 8: **Results of α-SVRG with AdamW on smaller datasets with standard deviation.**

In Section 5, we primarily use AdamW as the base optimizer in α-SVRG to study α-SVRG. Here we switch the base optimizer in α-SVRG from AdamW to SGD. Specifically, we train a ResNet-18 (He et al., 2016), which by default uses SGD to train, on the same eight image classification datasets as above (Table 8). Following He et al. (2016), we use an initial learning rate of 0.1, which is divided by 10 when the error plateaus, a momentum of 0.9, and a weight decay of 0.0001. Other training recipe remains the same as Table 5. Hyperparameters are illustrated in Table 6. We compare α-SVRG (α_0 = 0.5) equipped by a linear decreasing schedule to the baseline using only SGD.

	C-100	Pets	Flowers	STL-10	Food101	DTD	SVHN	EuroSAT
batch size	1024	128	128	128	1024	128	1024	512
training epochs	150	200	150	200	50	200	50	100

Table 9: **Hyper-parameter setting for SGD and α-SVRG on ResNet-18.**

The results, shown in Table 10, are based on the average of 3 runs with different random seeds. As we can see, α-SVRG consistently outperforms the SGD baseline across all datasets.

	CIFAR-100	Pets	Flowers	STL-10
SGD	3.118 ± 0.035	2.706 ± 0.095	2.822 ± 0.058	1.763 ± 0.032
+ α-SVRG	**3.087** ± 0.011	**2.655** ± 0.134	**2.699** ± 0.049	**1.725** ± 0.043
	Food-101	DTD	SVHN	EuroSAT
SGD	3.424 ± 0.015	2.589 ± 0.032	1.789 ± 0.029	1.449 ± 0.029
+ α-SVRG	**3.397** ± 0.006	**2.543** ± 0.039	**1.764** ± 0.014	**1.412** ± 0.011

(a) **training loss**

	CIFAR-100	Pets	Flowers	STL-10
SGD	75.43 ± 0.88	71.25 ± 4.74	65.92 ± 4.24	76.09 ± 1.09
+ α-SVRG	**75.93** ± 0.83	**71.89** ± 4.84	**74.98** ± 3.14	**78.55** ± 2.54
	Food-101	DTD	SVHN	EuroSAT
SGD	60.58 ± 2.00	57.53 ± 1.25	91.10 ± 1.31	95.31 ± 0.46
+ α-SVRG	**62.89** ± 0.87	**58.44** ± 1.05	**91.60** ± 0.59	**96.17** ± 0.17

(b) **validation accuracy**

Table 10: **Results of α-SVRG with SGD on smaller datasets with standard deviation.**

G THEORETICAL ANALYSIS

In this section, we prove that the convergence rate of α-SVRG is the same as vanilla SGD.

Setup. For clarity, we adopt the following notations: s as the epoch index, t as the iteration index within each epoch, i_t as the sampled index at iteration t, T as the epoch length, M as the iteration length within each epoch, n as the total number of training data, η_t^s as the learning rate, and α_t^s as the scalar coefficient value. Let $\boldsymbol{\theta}_t^s$ be the model parameters at epoch s and iteration t. Let f_i be the individual loss function for the i-th training data point and f be the loss function over the entire training data. We illustrate α-SVRG with SGD in Algorithm 1 and with AdamW in Algorithm 2:

Algorithm 1 α-SVRG with SGD$\big(\boldsymbol{\theta}_0^0, T, M, \{\{\eta_t^s\}_{t=0}^{M-1}\}_{s=0}^{T-1}, \{\{\alpha_t^s\}_{t=0}^{M-1}\}_{s=0}^{T-1}, \lambda\big)$

Input: initialized model parameters $\boldsymbol{\theta}_0^0$, epoch length T, iteration length within each epoch M, learning rates $\{\{\eta_t^s\}_{t=0}^{M-1}\}_{s=0}^{T-1}$, scheduled coefficients $\{\{\alpha_t^s\}_{t=0}^{M-1}\}_{s=0}^{T-1}$, weight decay λ
$\boldsymbol{\theta}_{\text{past}}^0 = \boldsymbol{\theta}_0^0$
for $s = 0$ **to** $T-1$ **do**
  $\nabla f(\boldsymbol{\theta}_{\text{past}}^s) = \frac{1}{n}\sum_{i=1}^n \nabla f_i(\boldsymbol{\theta}_{\text{past}}^s)$
  for $t = 0$ **to** $M-1$ **do**
    $i_t \overset{\text{iid}}{\sim} \text{Uniform}\{1, \cdots, n\}$
    $\boldsymbol{g}_t^s = \nabla f_{i_t}(\boldsymbol{\theta}_t^s) - \alpha_t^s \left(\nabla f_{i_t}(\boldsymbol{\theta}_{\text{past}}^s) - \nabla f(\boldsymbol{\theta}_{\text{past}}^s)\right)$
    $\boldsymbol{\theta}_{t+1}^s = \boldsymbol{\theta}_t^s - \eta_t^s \boldsymbol{g}_t^s - \lambda \boldsymbol{\theta}_t^s$
  end for
  $\boldsymbol{\theta}_{\text{past}}^{s+1} = \boldsymbol{\theta}_M^s$
end for
Output: final model $\boldsymbol{\theta}_M^{T-1}$.

Algorithm 2 α-SVRG with AdamW$\big(\boldsymbol{\theta}_0^0, T, M, \{\{\eta_t^s\}_{t=0}^{M-1}\}_{s=0}^{T-1}, \{\{\alpha_t^s\}_{t=0}^{M-1}\}_{s=0}^{T-1}, \beta_1, \beta_2, \lambda\big)$

Input: initialized model parameters $\boldsymbol{\theta}_0^0$, epoch length T, iteration length within each epoch M, learning rates $\{\{\eta_t^s\}_{t=0}^{M-1}\}_{s=0}^{T-1}$, scheduled coefficients $\{\{\alpha_t^s\}_{t=0}^{M-1}\}_{s=0}^{T-1}$, momentums β_1, β_2, weight decay λ
$\boldsymbol{\theta}_{\text{past}}^0 = \boldsymbol{\theta}_0^0$
$\boldsymbol{m} = \boldsymbol{v} = 0$
for $s = 0$ **to** $T-1$ **do**
  $\nabla f(\boldsymbol{\theta}_{\text{past}}^s) = \frac{1}{n}\sum_{i=1}^n \nabla f_i(\boldsymbol{\theta}_{\text{past}}^s)$
  for $t = 0$ **to** $M-1$ **do**
    $i_t \overset{\text{iid}}{\sim} \text{Uniform}\{1, \cdots, n\}$
    $\boldsymbol{g}_t^s = \nabla f_{i_t}(\boldsymbol{\theta}_t^s) - \alpha_t^s \left(\nabla f_{i_t}(\boldsymbol{\theta}_{\text{past}}^s) - \nabla f(\boldsymbol{\theta}_{\text{past}}^s)\right)$
    $\boldsymbol{m} = \beta_1 \boldsymbol{m} + (1-\beta_1)\boldsymbol{g}_t^s$
    $\boldsymbol{v} = \beta_2 \boldsymbol{v} + (1-\beta_2)(\boldsymbol{g}_t^s)^2$
    $\boldsymbol{\theta}_{t+1}^s = \boldsymbol{\theta}_t^s - \eta_t^s \frac{\boldsymbol{m}}{\sqrt{\boldsymbol{v}}+\epsilon} - \lambda \boldsymbol{\theta}_t^s$
  end for
  $\boldsymbol{\theta}_{\text{past}}^{s+1} = \boldsymbol{\theta}_M^s$
end for
Output: final model $\boldsymbol{\theta}_M^{T-1}$.

Convergence Analysis. Following prior work (Allen-Zhu & Hazan, 2016; Reddi et al., 2016; Lei et al., 2017), we hold the standard L-smooth assumption on each individual loss function f_i. That is there exists a constant L:

$$\forall i \in \{1, \cdots, n\}\ \forall \boldsymbol{\theta}_1, \boldsymbol{\theta}_2\ ||\nabla f_i(\boldsymbol{\theta}_1) - \nabla f_i(\boldsymbol{\theta}_2)|| \leq L||\boldsymbol{\theta}_1 - \boldsymbol{\theta}_2||. \tag{19}$$

The L-smooth assumption allows us to have the following important descent lemma:

$$\mathbb{E}[\nabla f(\boldsymbol{\theta}_{t+1}^s)] \leq \mathbb{E}[\nabla f(\boldsymbol{\theta}_t^s) + < \nabla f(\boldsymbol{\theta}_t^s), \boldsymbol{\theta}_{t+1}^s - \boldsymbol{\theta}_t^s > + \frac{L}{2}||\boldsymbol{\theta}_{t+1}^s - \boldsymbol{\theta}_t^s||^2]. \tag{20}$$

We also hold the σ-bounded gradient assumption on each individual loss function f_i. That is there exists a constant σ:

$$\forall i \in \{1, \cdots, n\} \; \forall \boldsymbol{\theta} \; ||\nabla f_i(\boldsymbol{\theta})|| \leq \sigma. \tag{21}$$

We first show the following bound on the variance reduced gradient $\boldsymbol{g}_t^s$:

$$\begin{aligned}
\mathbb{E}[||\boldsymbol{g}_t^s||^2] &= \mathbb{E}[||\nabla f_{i_t}(\boldsymbol{\theta}_t^s) - \alpha_t^s(\nabla f_{i_t}(\boldsymbol{\theta}_0^s) - \nabla f(\boldsymbol{\theta}_0^s))||^2] && (22)\\
&\leq 2\mathbb{E}[||\nabla f_{i_t}(\boldsymbol{\theta}_t^s)||^2 + ||\alpha_t^s(\nabla f_{i_t}(\boldsymbol{\theta}_0^s) - \nabla f(\boldsymbol{\theta}_0^s))||^2] && (23)\\
&\leq 2\mathbb{E}[||\nabla f_{i_t}(\boldsymbol{\theta}_t^s)||^2 + (\alpha_t^s)^2||\nabla f_{i_t}(\boldsymbol{\theta}_0^s)||^2] && (24)\\
&\leq (2 + \frac{2}{TM}\sum_{s,t}(\alpha_t^s)^2)\sigma^2 && (25)\\
&\leq 4\sigma^2. && (26)
\end{aligned}$$

The first inequality is from $\mathbb{E}[||X - Y||^2] \leq 2\mathbb{E}[||X||^2 + ||Y||^2]$. The second inequality is from $\mathbb{E}[||X - \mathbb{E}[X]||^2] \leq \mathbb{E}[||X||^2]$. The third inequality is from the σ-bounded gradient assumption. The last inequality is from the fact that our coefficients are always between 0 and 1: $\forall s, t, \; \alpha_t^s \in [0, 1]$.

We then proceed to prove our main result. From the descent lemma (Equation 20) and variance bound on the variance reduced gradient $\boldsymbol{g}_t^s$ (Equation 26), we can show:

$$\begin{aligned}
\mathbb{E}[\nabla f(\boldsymbol{\theta}_{t+1}^s)] &\leq \mathbb{E}[\nabla f(\boldsymbol{\theta}_t^s) + < \nabla f(\boldsymbol{\theta}_t^s), \boldsymbol{\theta}_{t+1}^s - \boldsymbol{\theta}_t^s > + \frac{L}{2}||\boldsymbol{\theta}_{t+1}^s - \boldsymbol{\theta}_t^s||^2] && (27)\\
&\leq \mathbb{E}[\nabla f(\boldsymbol{\theta}_t^s)] - \eta_t^s\mathbb{E}[||\nabla f(\boldsymbol{\theta}_t^s)||^2] + \frac{L(\eta_t^s)^2}{2}\mathbb{E}[||g_t^s||^2] && (28)\\
&\leq \mathbb{E}[\nabla f(\boldsymbol{\theta}_t^s)] - \eta_t^s\mathbb{E}[||\nabla f(\boldsymbol{\theta}_t^s)||^2] + 2L(\eta_t^s)^2\sigma^2. && (29)
\end{aligned}$$

We can then rearrange it as a bound on the square of the gradient norm:

$$\mathbb{E}[||\nabla f(\boldsymbol{\theta}_t^s)||^2] \leq \frac{1}{\eta_t^s}\mathbb{E}[\nabla f(\boldsymbol{\theta}_t^s) - \nabla f(\boldsymbol{\theta}_{t+1}^s)] + 2L\eta_t^s\sigma^2. \tag{30}$$

We then average the inequality over the entire optimization trajectory:

$$\begin{aligned}
\min_{s,t}\mathbb{E}[||\nabla f(\boldsymbol{\theta}_t^s)||^2] &\leq \frac{1}{TM}\sum_{t,s}\mathbb{E}[||\nabla f(\boldsymbol{\theta}_t^s)||^2] && (31)\\
&\leq \frac{1}{TM\eta_t^s}(\nabla f(\boldsymbol{\theta}_0^0) - \nabla f(\boldsymbol{\theta}_M^{T-1})) + 2L\eta_t^s\sigma^2 && (32)\\
&\leq \frac{1}{TM\eta_t^s}(\nabla f(\boldsymbol{\theta}_0^0) - \nabla f(\boldsymbol{\theta}^*)) + 2L\eta_t^s\sigma^2, && (33)
\end{aligned}$$

where $\boldsymbol{\theta}^*$ is the global minimizer of the loss function f. The first inequality follows from the fact that the minimum of a set of non-negative numbers is always smaller than their average.

We can then set η_t^s to be:

$$\eta_t^s = \sqrt{\frac{\nabla f(\boldsymbol{\theta}_0^0) - \nabla f(\boldsymbol{\theta}^*)}{2LTM\sigma^2}}, \tag{34}$$

so that the inequality becomes :

$$\min_{s,t}\mathbb{E}[||\nabla f(\boldsymbol{\theta}_t^s)||^2] \leq 2\sqrt{\frac{2L(\nabla f(\boldsymbol{\theta}_0^0) - \nabla f(\boldsymbol{\theta}^*))}{TM}}\sigma. \tag{35}$$

Thus, α-SVRG requires at most $O(\frac{1}{\epsilon^2})$ iteration steps to achieve ϵ-accuracy solution $\mathbb{E}[||\nabla f(\boldsymbol{\theta}_t^s)||^2] \leq \epsilon$. This guarantees the convergence rate of α-SVRG will not be worse than SGD.

H CONVERGENCE COMPARISON

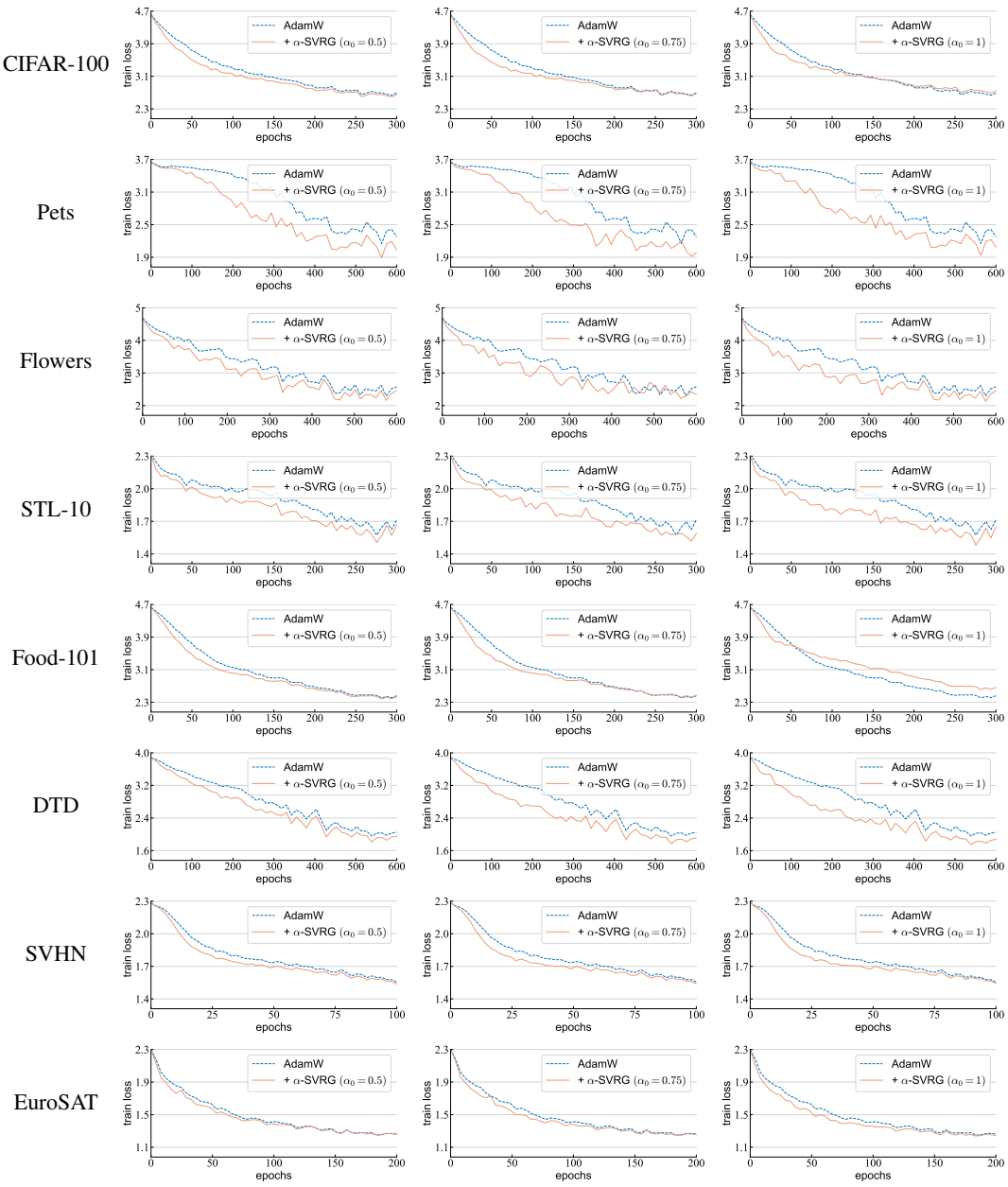

Figure 15: **Training loss with AdamW and α-SVRG on smaller classification datasets (Table 7).**

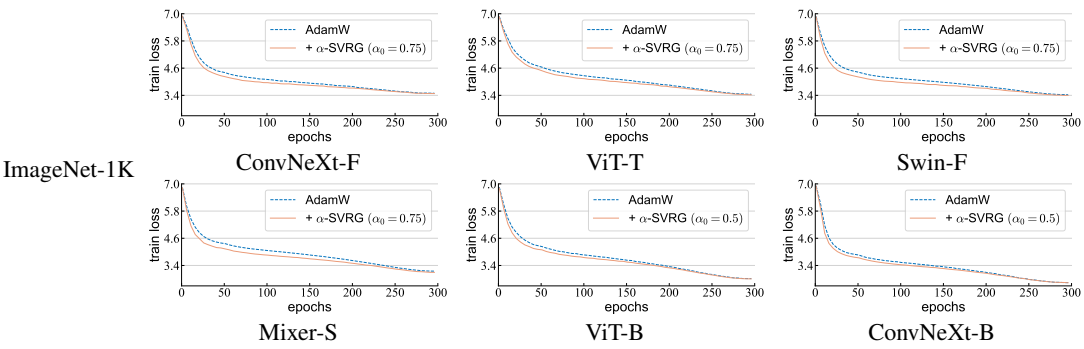

Figure 16: **Training loss with AdamW and α-SVRG on ImageNet-1K (Table 2).**

I LIMITATIONS

In this work, we have shown α-SVRG can optimize models better by reducing gradient variance. Nevertheless, just like the standard SVRG, it requires about $2\times$ additional computation cost compared to vanilla SGD or AdamW because it needs to calculate both the snapshot full gradient $\nabla f(\boldsymbol{\theta}^{\text{past}})$ and the snapshot stochastic gradient $\nabla f_i(\boldsymbol{\theta}^{\text{past}})$ between two consecutive snapshot captures. We can reduce this to $1\times$ by storing the individual snapshot stochastic gradient $\nabla f_i(\boldsymbol{\theta}^{\text{past}})$ in the memory when calculating the snapshot full batch gradient $\nabla f(\boldsymbol{\theta}^{\text{past}})$ at the beginning of each epoch.

J Additional Results of α-SVRG

J.1 Different Learning Rates

α-SVRG with AdamW. In Section 5, we use the same base learning rate of 4e-3 for both AdamW and α-SVRG. However, each method's optimal learning rate might be different. Here we sweep the base learning rate over the range $\{$1e-2, 5e-3, 1e-3, 5e-4, 1e-4$\}$ and compare α-SVRG ($\alpha_0 = 0.5$) to AdamW in Figure 17. The results show α-SVRG can decrease training loss better than vanilla AdamW in most cases.

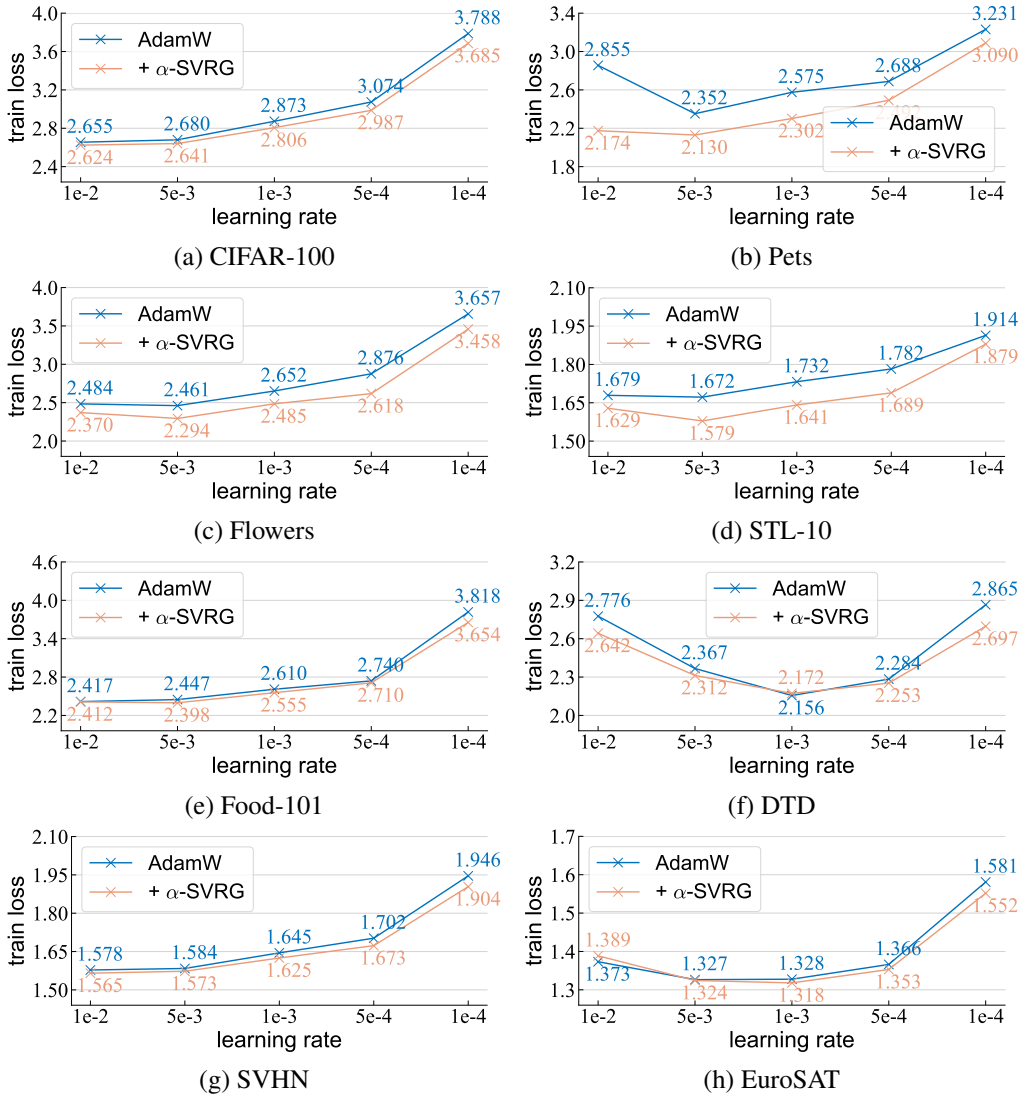

(a) CIFAR-100 (b) Pets

(c) Flowers (d) STL-10

(e) Food-101 (f) DTD

(g) SVHN (h) EuroSAT

Figure 17: α-SVRG can achieve a lower training loss than AdamW at different learning rates.

α-SVRG with SGD. We also sweep the base learning rate for the results of Table 10 using SGD as the base optimizer. We compare vanilla SGD to α-SVRG ($\alpha_0 = 0.5$). The results are shown in Figure 18. In most cases, α-SVRG can achieve a lower training loss than SGD.

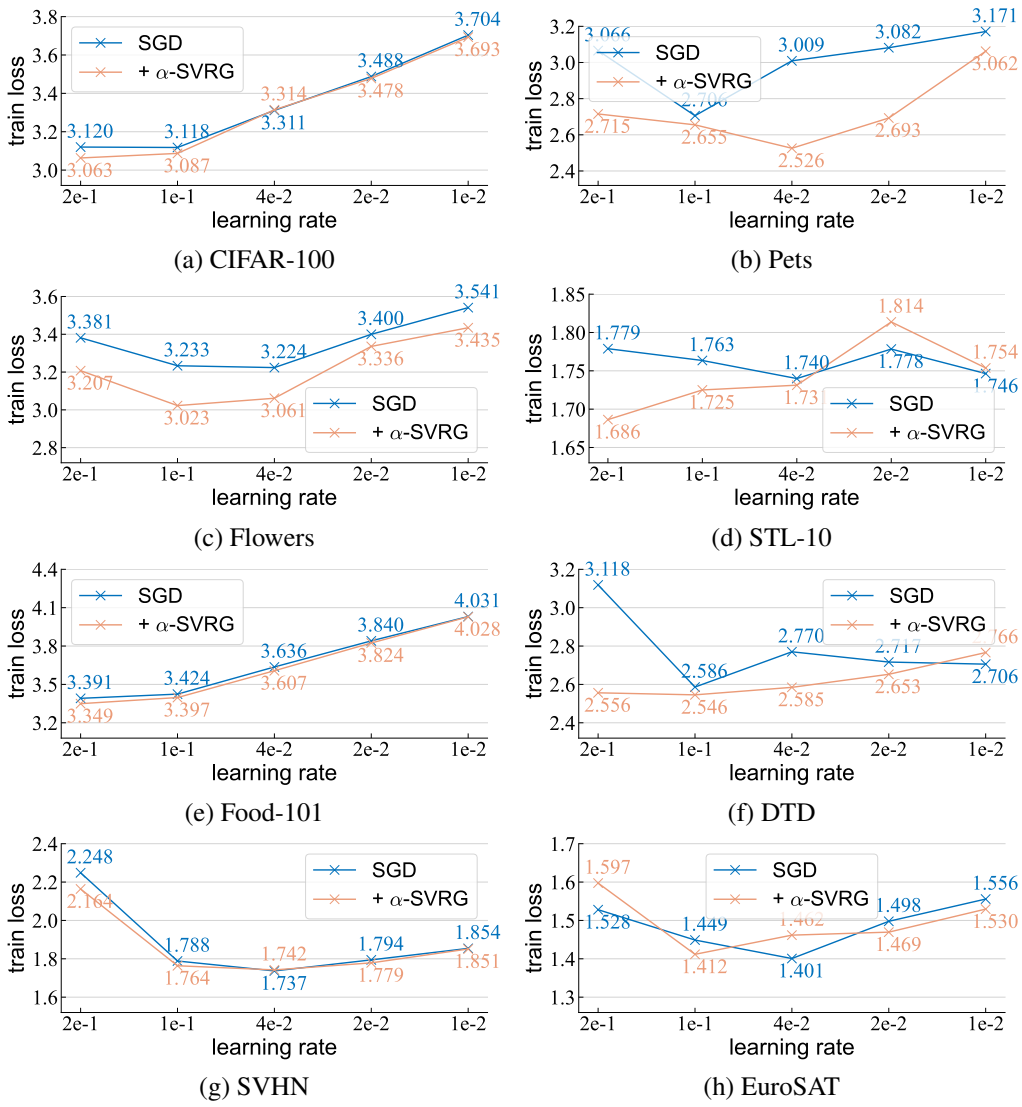

Figure 18: α-SVRG can achieve a lower training loss than SGD at different learning rates.

J.2 EARLY α-SVRG

Compared with baseline methods like SGD and AdamW, both standard SVRG and α-SVRG require computing the snapshot stochastic gradient $\nabla f_i(\boldsymbol{\theta}^{\text{past}})$ and snapshot full gradient $\nabla f(\boldsymbol{\theta}^{\text{past}})$. This usually results in about twice the computational cost of the baseline methods. Nevertheless, as observed in Section 4, α-SVRG effectively reduces gradient variance during the initial training epochs and then maintain at a similar level as the baseline methods. This leads us apply α-SVRG only at the early phases of training, and we refer this approach as early α-SVRG.

	CIFAR-100		Pets		Flowers		STL-10	
AdamW	2.659	-	2.203	-	2.400	-	1.641	-
+ α-SVRG	2.646	↓0.013	2.004	↓0.199	2.162	↓0.238	1.568	↓0.073
+ early α-SVRG	2.644	↓0.015	2.190	↓0.013	2.328	↓0.072	1.616	↓0.025
	Food-101		DTD		SVHN		EuroSAT	
AdamW	2.451	-	1.980	-	1.588	-	1.247	-
+ α-SVRG	2.461	↑0.010	1.829	↓0.151	1.573	↓0.015	1.237	↓0.010
+ early α-SVRG	2.444	↓0.007	1.918	↓0.062	1.583	↓0.005	1.240	↓0.007

(a) **training loss**

	CIFAR-100		Pets		Flowers		STL-10	
baseline	81.0	-	72.8	-	80.8	-	82.3	-
+ α-SVRG	80.6	↓0.4	76.7	↑3.9	82.6	↑1.8	84.0	↑1.7
+ early α-SVRG	81.0	↑0.0	74.6	↑1.8	83.6	↑2.8	82.8	↑0.5
	Food-101		DTD		SVHN		Euro	
baseline	85.9	-	57.9	-	94.9	-	98.1	-
+ α-SVRG	85.0	↓0.9	60.3	↑2.4	95.7	↑0.8	98.2	↑0.1
+ early α-SVRG	85.9	↑0.0	62.3	↑4.4	95.8	↑0.9	98.0	↓0.1

(b) **validation accuracy**

Table 11: **Early α-SVRG on smaller classification datasets.**

To evaluate this approach, we use early α-SVRG to optimizer ConvNeXt-Femto on various image classification datasets. Specifically, α-SVRG is applied during the first 10% of training and is disabled thereafter. The scheduling of the coefficient ($\alpha_0 = 0.75$) follows the default linear decay pattern, with an added transition epoch where the coefficient decreases from its current value to zero. Empirically, we find this transition epoch crucial for maintaining the stability of momentum in the base optimizer.

Figure 11 shows the results. Early α-SVRG can consistently reduce training loss across different datasets. Furthermore, we observe that the validation accuracy achieved by early α-SVRG sometimes surpasses that of standard α-SVRG. This phenomenon is likely because disabling α-SVRG in the later training stages allows the presence of benign gradient noise during optimization. Such noise may drive the model toward local minima that exhibit better generalization properties (Smith et al., 2020; Damian et al., 2021; Li et al., 2022).

K ADDITIONAL RESULTS OF OPTIMAL COEFFICIENT

K.1 EFFECTS OF DATA

In Section 3, we show a deeper model has a smaller optimal coefficient. Here, we analyze how data affects optimal coefficient during the training. Specifically, we train 1, 2, and 4-layer MLPs (Logistic Regression, MLP-2, and MLP-4) on CIFAR-10 and CIFAR-100 using SGD and compute the optimal coefficient (Equation 6). Figure 19 shows the results.

The optimal coefficient of each model trained on CIFAR-10 is lower than that on CIFAR-100. This is possibly because CIFAR-100 has 10x object classes than CIFAR-10 and therefore the correlation

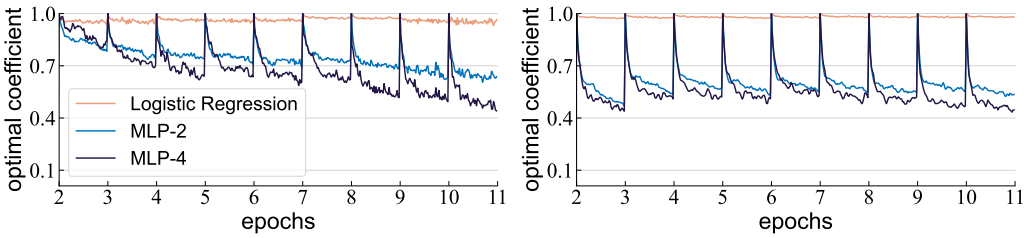

(a) CIFAR-10 (b) CIFAR-100

Figure 19: **Effects of Data on Optimal Coefficient.**

between the snapshot model gradient and the current model gradient is lower. Thus, we recommend using a smaller coefficient when the training dataset includes a larger number of classes.

K.2 SVRG WITH OPTIMAL COEFFICIENT

Throughout the experiments in Section 3, we mainly study the behavior of SVRG with optimal coefficient on CIFAR-10 dataset. To show the generality of this method, we below study it on other image classification datasets. We train a MLP-4 on Flowers / EuroSAT with SGD and SVRG with optimal coefficient for 15 / 12 epochs. As shown in Figure 20, SVRG with optimal coefficient can consistently reduce gradient variance and achieve a lower training loss than the baseline SGD.

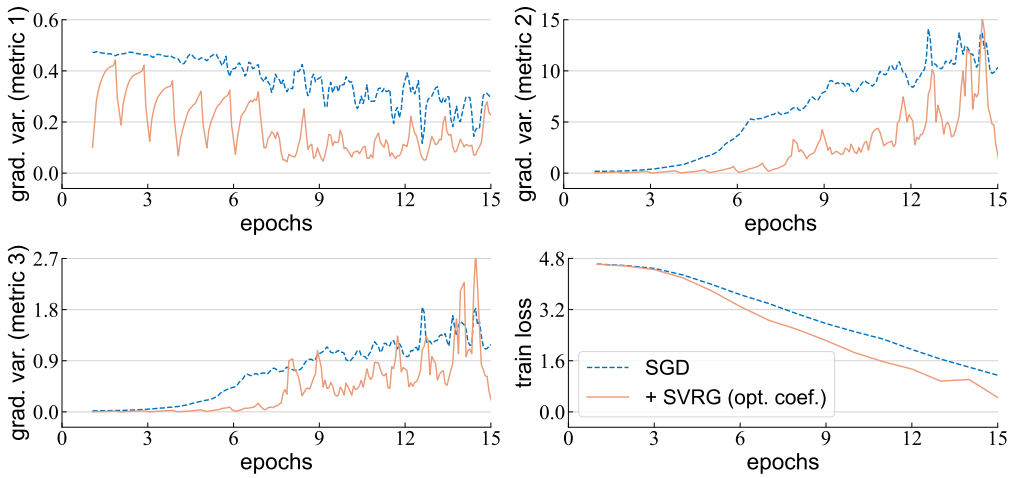

(a) Flowers

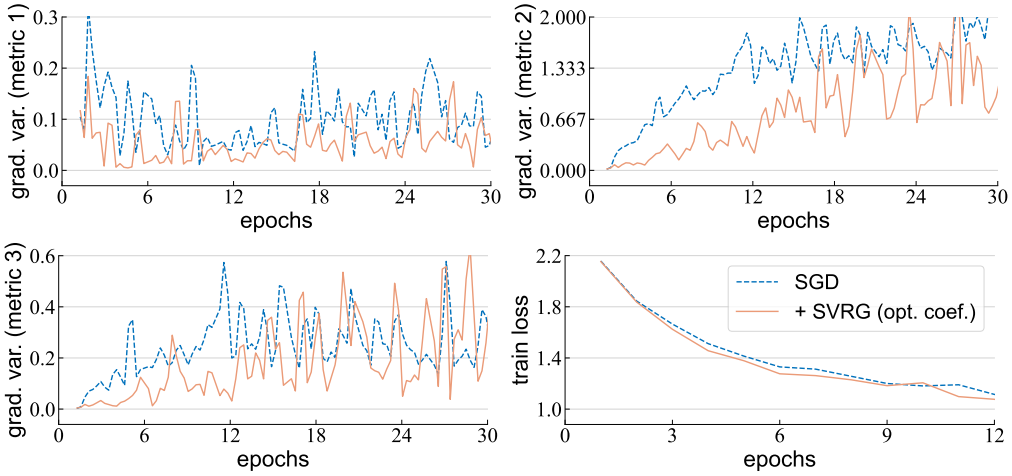

(b) EuroSAT

Figure 20: **SVRG with optimal coefficient on other datasets.**